2022

Improving Quantification of Mitral Regurgitation Through Computational Fluid Dynamics and Ex Vivo Testing

Alexandra Flowers
University of Denver

Improving Quantification of Mitral Regurgitation through Computational Fluid Dynamics and Ex Vivo Testing

---

A Thesis

Presented to

the Faculty of the Daniel Felix Ritchie School of Engineering and Computer Science

University of Denver

In Partial Fulfillment

of the Requirements for the Degree

Master of Science

---

by

Alexandra Flowers

March 2022

Dr. Ali N. Azadan

Author: Alexandra Flowers
Title: Improving Quantification of Mitral Regurgitation through Computational Fluid Dynamics and Ex vivo Testing
Advisor: Dr. Ali N. Azadani
Degree Date: March 2022

Abstract

Mitral regurgitation (MR) is a prominent cardiac disease affecting more than two million people in the United States alone. In order for patients to receive proper therapy, regurgitant volume must first be quantified. As there are an array of methods to do so, the proximal isovelocity surface area (PISA) method continues to be the most accurate and clinically used method. However, there are some difficulties obtaining the necessary measurements need for this when performing transthoracic echocardiography. This study aims to evaluate and present techniques that may be used to more accurately quantify regurgitation through ex vivo testing and computational fluid dynamic simulations. Both a steady and pulsatile flow system were created to test clinical applications used to quantify MR using the PISA method. A total of six computational fluid dynamic cases were then studied; three native mitral valves effected by MR as well as three valves enacting to have MitraClip implantation, both sets of having a MR grade of mild, moderate, and severe. All cases were effected by an eccentric ellipse orifice(s). Flow rate was evaluated in each case, comparing actual flow rate to calculated flow rate, which was found implementing the modified hemielliptic PISA model. The results of this study implicate that clinical techniques used to quantify MR need an experienced technician, as well as further developing current techniques used, which is best done through ex vivo testing. The study further implied that severity may be significantly underestimated when quantifying MR using the modified hemielliptic PISA method in the short view.

Acknowledgements

First and foremost, I would like to thank my research advisor, Dr. Ali Azadani, for his invaluable guidance, generosity, encouragement, and patience throughout the course of my Master's program. Through showing me all that Cardiovascular Biomechanics and academia has to offer, you have shown me a field I am truly passionate about and wish to continue to pursue. I would like to thank the Faculty Research Fund Grant for giving us the opportunity to build our full cardiac simulator. I would also like to thank my lab mate Dong Qui for his continuous support, positivity, and friendship over the years, helping to make my research experience that much better.

Additionally, I would like to thank Dr. Breigh Roszelle for being a mentor over the years, Justin Huff for his assistance to build our simulator, Gabrielle Kindy for her help with computer modeling and experimental testing, and Mina Shafiei for her help with experimental testing. Last but not least, I would like to say thank you to all my friends and family for their continued support and infectious optimism; truly making my academic years enjoyable!

Table of Contents

Chapter One:
Introduction……...1
1.1 Mitral Valve Anatomy……2
1.1.1Leaflets…….…….3
1.1.2 Chordae Tendineae……...3
1.1.3 Papillary Muscle……...4
1.2 Mitral Regurgitation Prognosis; Etiology & Pathophysiology ……...5
1.2.1 Primary MR……..5
1.2.2 Secondary MR……..6
1.3 Assessment of Mitral Regurgitation ……...6
1.3.1 Cardiac Magnetic Resonance Imaging……7
1.3.2 Transesophageal Echocardiography ……8
1.3.3 Transthoracic Echocardiography ……9
1.3.3.1 Pulsed Wave Doppler……...10
1.3.3.2 Continuous Wave Doppler……...10
1.3.3.3 Color Doppler……...11
1.4 Quantification of Mitral Regurgitation Severity ……...11
1.4.1 Regurgitation Jet Area ……12
1.4.2 Vena Contracta ……...13
1.4.3 Flow Convergence; Proximal Isovelocity Surface Area ……13
1.5 Treatment of Mitral Regurgitation……14
1.5.1 Surgical Valve Replacement ……..15
1.5.2 Surgical Valve Repair ……16
1.5.3 MitraClip Implantation……...17
1.6 Simulated Cardiovascular Biomechanics……..19
1.7 Cardiac Simulators and Ex vivo Testing……...19
1.8 Research Aims ……..21

Chapter Two: Methods……23
2.1 Ex vivo Testing ……23
2.1.1 Steady Flow Design ……..23
2.1.2 Pulsatile Flow Design ……...25
2.1.3 Full Cardiac Simulator Construction……26
2.2 Experimental Subjects ……27
2.3 Transthoracic Echocardiography Techniques……28
2.3.1 Mitral Regurgitation Parameters / MR TTE methods……...28
2.4 Computational Fluid Dynamics ……...31
2.4.1 Model ……31
2.4.1.1 Native Mitral Regurgitation Valve ……32
2.4.1.2 MitraClip Implantation in Mitral Regurgitation Valve …….32
2.4.2 Mesh ……..33
2.4.3 ANSYS Fluent Simulation ……33
2.4.4 Simulated Echocardiography……34

2.5 Quantification of Severity ; Modified-Hemielliptic PISA Method ……...35
Chapter Three: Results ……37
3.1 Experimental Testing ……37
3.2 Computational Fluid Dynamics ; Simulation Contours…….47
3.3 Quantification of Mitral Regurgitation ; Modified Hemielliptic PISA …….53

Chapter Four: Discussion…….58
4.1 Ex vivo Testing……..58
4.2 Computational Fluid Dynamics…….58
4.3 Study Limitations & Future Works……60
4.3.1 Ex vivo Testing……...60
4.3.2 Computational Fluid Dynamics……..60

Chapter Five: Conclusions……...62

References ……...63

Appendix A……..68

List of Figures

Figure 1.1.1: Anatomy of Mitral Valve ……3
Figure 1.1.2: Mitral Valve Apparatus ……...……4
Figure 1.1.3: Carpentier's Classification of Mitral Regurgitation……6
Figure 1.4.1: Depiction of PISA shell…….…..…14
Figure 1.5.1: Depiction of MitraClip implantation …….……17
Figure 1.5.2: MitraClip apparatus ……...……18
Figure 1.7.1: Representation of Left Heart Simulator ……20

Figure 2.1.1.1: Steady Flow System Schematic ……..…24
Figure 2.1.1.2: Steady Flow System Design ……..……24
Figure 2.1.2.1: Full Cardiac Simulator Schematic …….……25
Figure 2.1.2.2: Full Cardiac System Design……26

Figure 3.1.1: Pig Heart Preparation Photo …….……38
Figure 3.1.2: Mitral Valve Sutured Photo……...……38
Figure 3.1.3: Pig Heart Prepared for Flow System Photo……...…39
Figure 3.1.4: Experimental Steady Flow System Photo…….39
Figure 3.1.5: Experimental Steady Flow with Pig Heart Photo…….40
Figure 3.1.6: Optimal Transducer Placement Photos…….41
Figure 3.1.7: Apical Cannula CAD Models……...…42
Figure 3.1.8: Compliance Chamber CAD Model……...……43
Figure 3.1.9: Reservoir CAD Model……...…44
Figure 3.1.10: Pig Heart Connection for Full Cardiac Simulator Photo……45
Figure 3.1.11: Full Cardiac Simulator Photo……..…45
Figure 3.1.12: Experimental Pressure Data……...……46
Figure 3.1.13: Experimental DICOM Images ……...…47
Figure 3.2.1: Native Mitral Valve CAD Models……..…….48
Figure 3.2.2: MitraClip Mitral Valve CAD Models …….48
Figure 3.2.3: Left Heart CAD Model…….……49
Figure 3.2.4: Left Heart Meshed Model……50
Figure 3.2.5 Simulated Flow through Left Heart Model Image……52
Figure 3.2.6: Native Mitral Valve Velocity Contours……52
Figure 3.2.7: MitraClip Mitral Valve Velocity Contours…….53
Figure 3.3.1: PISA Shell Radial Measurement ……54
Figure 3.3.2: PISA Shell Angle Measurement …….54
Figure 3.3.3: Simulated Flow Rates in Short Axis View……..57
Figure 3.3.4: Simulated Flow Rates in Long Axis View …….57

List of Tables

Table 2.4.1.1: Simulated Native Mitral Valve Orifice Details ……32
Table 2.4.1.2: Simulated MitraClip Mitral Valve Orifice Details …….....32

Table 3.1.1: Optimal Steady Flow System Techniques ……...42
Table 3.1.2: Optimal Full Cardiac Simulator Techniques ……...46
Table 3.2.1: Mesh Element Details ……..…50
Table 3.2.2: Simulated Boundary Condition Details……...51
Table 3.3.1: Native Mitral Valve Simulation Data …….……55
Table 3.3.2: MitraClip Mitral Valve Simulation Data…….……56

Chapter One: Introduction

Mitral regurgitation (MR) is the most common valvular heart disease known, having substantial prominence of morbidity and mortality in cardiac disease. As to prevent left ventricular dysfunction, heart failure, and a lower quality of life, MR warrants nearly 30,000 patients in the United States to undergo vital surgeries annually.[11; 13; 18] This prognosis is often due to functional impairment, anatomic integrity, and insidious progression. When first evaluating MR, it is important to examine patient etiology, mechanism, and pathology. MR must then be further evaluated in order to classify the cause of regurgitation and quantify severity, comparing this preliminary data to standard baseline measurements. Once severity has been determined, a cardiac team is able to determine a course of treatment.

Although there currently are baseline standards used in clinical practice as to how to quantify MR, the absence of a gold standard methodology remains to be a great difficulty. It is prevalent to have quantification methods be accurate as possible; if not regurgitant volume can be misconstrued, leading to erroneous course of treatment recommendations and decisions.[9] The treatment of mitral valve regurgitation can be further advanced through clinical assessment methods, mathematical models implemented, device development, patient-specific simulations, and ex vivo testing with biologic simulators.

1.1 Mitral Valve Anatomy

In order for the mitral valve to perform optimally, there must be near perfect function of the intricate relationship between the mitral leaflets, subvalvular structure, mitral annulus, and the left ventricle. Any deformity can cause the valve to leak and for regurgitation to occur. It is imperative to understand the anatomy of the mitral valve in order to evaluate not only the mechanism of a healthy valve, but also the etiology of a deformed valve to diagnosis regurgitation cause and severity.[14] The mitral valve is located in the left chamber of the heart between the left atrium and the left ventricle. Its overall structure includes the mitral annulus, mitral leaflets, chordae tendineae, and papillary muscles. The mitral annulus is bimodal in shape with the anterior and posterior leaflets superiorly positioned, and the medial and lateral points positioned inferiorly.

1.1.1 Leaflets

There are two mitral valve leaflets that help to make up the valve, referred to as the anterior and posterior leaflets. The anterior leaflet accounts for a much larger portion of surface area than the posterior leaflet and is connected to the noncoronary and left aortic cusps.[18] The posterior leaflet is semicircular shaped with three scalloped segments that are distinct through thin clefts between them. Both leaflets are attached to the anterior and posterior commissure. The scalloped parts of the both leaflets are labeled 1 through 3; 1 being connected to the anterolateral portion, 2 being the middle scallop, and 3 being connected to the posteromedial portion. They are then referred to as A1, A2, A3 and P1, P2, P3.[18]

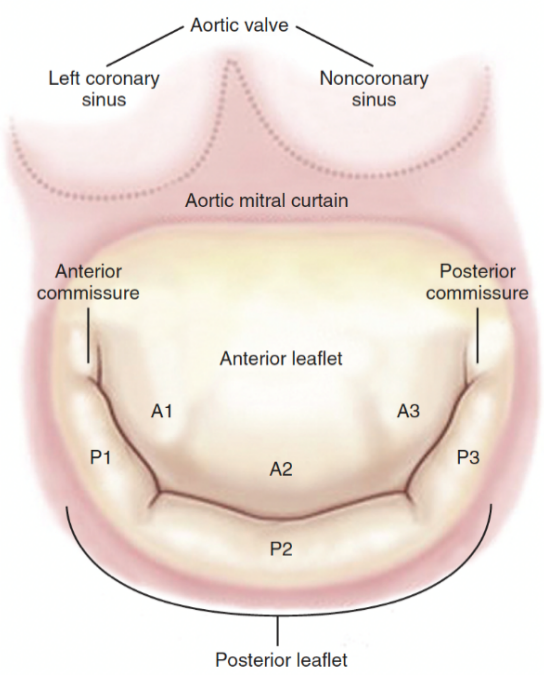

Figure 1.1.1: Mitral valve schematic view from atrial position. Anterior and posterior leaflets show scallops with specific numbers for each, allowing for detailed description of anatomy.[18]

1.1.2 Chordae Tendineae

The mitral chordae tendineae are fibrous structures made up of woven collagen and elastin fibers, and extend from the mitral leaflets to attach to the papillary muscles.[18] They serve to anchor the leaflets during systole and help to prevent prolapse of the leaflets into the left atrium. There are three types of chordae; primary, secondary, and tertiary. The primary chordae serves to maintain coaptation of the leaflets, extend to the papillary muscle in a branch-like fashion, and attaching to the coaptation line. The

secondary chordae serve to give support and length from the papillary muscle to the leaflets. They attach at the middle of the leaflets and are not branch-like, but are much thicker and longer than primary chordae.[18] Tertiary chordae give structural support and are attached to the leaflets from the basal myocardium.

1.1.3 Papillary Muscle

The two papillary muscles, the anterolateral and the posteromedial, connect the chordae to the left ventricle. The papillary muscles cause contraction of the chordae and leaflets during systole. There is an equal amount of chordae that extends from the papillary muscles to the leaflets, with the anterolateral papillary muscle / chordae attaching to medial half of the leaflets and the posteromedial muscle / chordae attaching to the lateral half of the leaflets.[18]

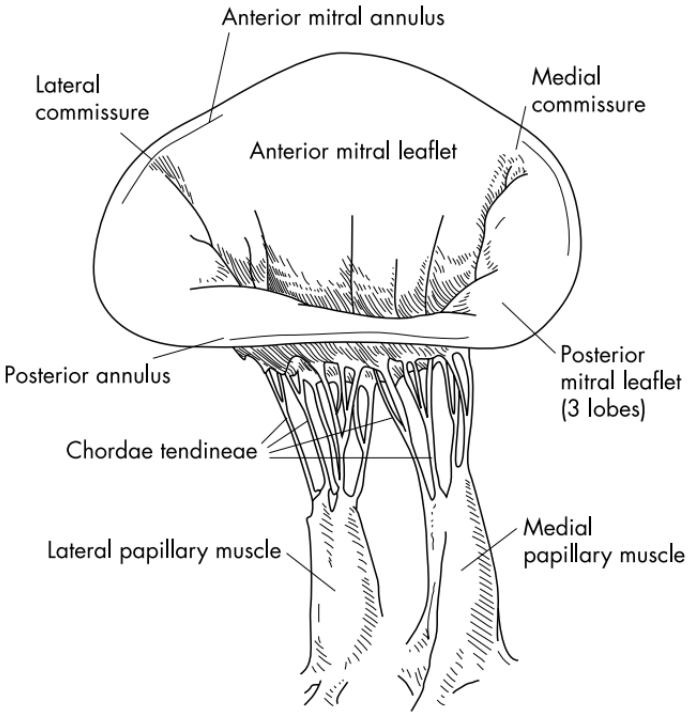

Figure 1.1.2: Description of full mitral valve apparatus.[14]

1.2 Epidemiology & Pathophysiology of Mitral Valve

Determining etiology of the mitral valve is most commonly done through transthoracic echocardiography (TTE).[13] MR is originally classified as primary or secondary. Primary MR is due to valvular dysfunction, whereas secondary (functional) MR is due to abnormalities in the subvalvular structure and / or the left ventricle.[9; 18] All abnormalities of the mitral valve, left atrium, and left ventricle should be noted in detail when being examined (i.e. size, location, extremity). As primary and secondary mitral regurgitation are considered different diseases, it is imperative that different methods are used for assessment, quantification, and course of treatment.[13]

1.2.1 Primary MR

Irregularities that occur in the leaflets are thickening, calcification, redundancy, perforation, vegetations, and clefts. Left chamber dilation is an indicator that MR is chronic and potentially severe.[13] Primary MR is further determined based on Carpentier's classification of leaflet motion, as Type I (normal leaflet motion), Type II (excessive motion), and Type III (restrictive motion).[9] Prolapse is the most common type of primary MR, caused by the dislocation / flail of the mitral leaflets during systole. Flail leaflet is the inversion of the leaflet and distorting the natural concave shape of the leaflet and is often a due to rupture of the primary chordae, giving loss of leaflet coaptation.[18] Other causes of primary MR are infection (endocarditis and leaflet perforations), inflammation (thickening of leaflets and poor coaptation), rheumatic disease (leaflet scarring and restricted leaflet motion), and radiation / drug induced (valvulitis and mitral stenosis).[18]

1.2.2 Secondary MR

Deformities causing functional MR include chordal rupture, thickening, fusion, vegetations, and masses. A dilated left ventricle with isolated wall abnormalities can help to identify severe secondary MR.[13] Secondary MR occurs from ischemic and myopathic left ventricle alteration, regardless if the valve is healthy or not, effecting the papillary muscles and mitral leaflet coaptation.[9; 18] Secondary MR is more common than primary MR, as ischemic cardiovascular diseases are more common than valvular etiology. Ischemic results from coronary artery disease and can also be caused by acute myocardial ischemia.[18]

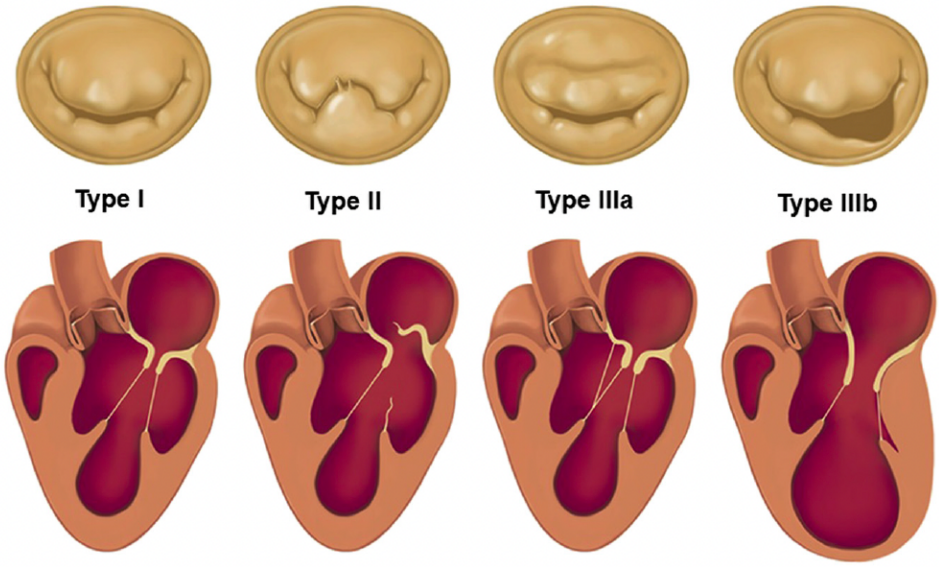

Figure 1.1.3: Anatomic description of Carpentier's classification of mitral regurgitation.[2]

1.3 Assessment of Mitral Regurgitation

Mitral regurgitation is typically first detected in asymptomatic patients through a systolic murmur found during an echocardiogram procedure.[14] Regurgitation occurring in

the mitral valve is assessed through two types of echocardiograms; transesophageal echocardiography (TEE) or TTE. Echocardiography is used to take images of the heart in real-time, to help evaluate the structure of the etiology, physiology, and hemodynamics.[13; 22] TEE procedures are performed by cardiologists and are often used if the data found from a TTE exam, performed by a sonographer, is ambiguous.[13] Initially, it is important for the clinical team to note all abnormalities found in detail in order to help determine and classify the type of MR present.[16] Patients showing signs of mild MR are recommended to have less frequent examinations, about once every five years, where as patients showing signs of moderate to severe MR are recommended to have an annual exam.[14] MR may also be assessed through non-cardiographic methods, such as computed tomography (CT), cardiovascular magnetic resonance (CMR), and angiography, but TEE and TTE are shown as the most accurate practices used.[22] Once MR has been classified, further investigation is need to more accurately quantify the level of severity. As there is not a single procedure for this, the American Society of Echocardiography (ASE) recommends an integrated approach using many parameters to do so.[18] This consists of an experienced cardiac / clinical team performing the suitable echocardiogram, and obtaining these images / measurements to be further used in mathematical modalities used to accurately quantify regurgitant volume.

1.3.1 Cardiac Magnetic Resonance Imaging

Cardiac magnetic resonance imaging (CMR) is a non-invasive assessment method used to take images of the heart in real-time, displaying cardiac dysfunction. This

can also be used as another option to help quantify regurgitation severity, as images taken are able to depict regurgitant orifice area, regurgitant volume, regurgitant fraction, and LV volume, indicating remodeling that has taken place.[1; 7] These measurements have shown to correspond with data from other methods, such as Doppler, but there are still quite a few disadvantages. Some major limitations with CMR is the lack of accessibility, cost of the procedure, inability to account for hemodynamics, and difficulty aligning the image with the most narrow part of the vena contracta.[7] Although this method can help to quantify regurgitation, it should mainly be used as a back up method for patients where TEE is not optimal, and where TTE data shows to be inconclusive.[1; 22]

1.3.2 Transesophageal Echocardiography

Transesophageal echocardiography is a type of echocardiogram that requires patient sedation, as an ultrasonic transducer is inserted through the esophagus in order to take images of the heart in real time.[1] TEE is known for giving generally the best overall assessment of mechanism abnormalities (I.e. leaflet prolapse / restriction) and the lesion causing regurgitation (I.e. chordae tendineae rupture, papillary muscle rupture, leaflet perforation, etc.).[1; 22] Whether or not MR is acute or chronic, as well as the chambers capacity to adjust for the regurgitant flow, is also evaluated.[23] Severity quantification methods are also able to be performed through data gathered from TEE, however there are some limitations. As regurgitant jet size is affected by transducer pulse repetition frequency (PRF) and the strength of the transducer signal, which may overestimate jet size.[23] Though somewhat faultless images and quantitative data is able to be taken through TEE, it is often avoided if possible due to patient risks as it is somewhat an

invasive procedure.[1; 23] TEE is best used as a second option if the data taken shows to be inconclusive and as a method for planning surgical repair / replacement.[16; 23]

1.3.3 Transthoracic Echocardiography

Transthoracic echocardiography (TTE) is the most common assessment approach when evaluating valvular regurgitation as it is a non-invasive procedure and there are various techniques to do so. This is done by placing an ultrasonic transducer on the abdomen / chest to capture images of the heart. A great advantage of TTE is that there is no affect on the hemodynamics unlike TEE.[1] This procedure is performed by a trained sonographer. 2D echocardiography helps to evaluate valvular structure and the impact of volume overload in the cardiac chambers in present time through a single slice / two-dimensional image.[23] 3D echocardiography is able to give a more complex image of the mitral valve apparatus through the perspective of the left atrium (LA and left ventricle (LV).[7] Anatomic and functional abnormalities are also evaluated through this type of echocardiogram. An advantage of a 3D echocardiograms is the ability to not rely on geometric postulations when measuring the regurgitant orifice area, which is needed in a 2D echocardiogram.[7] Doppler echocardiography is another type of echocardiogram that uses high frequency ultrasonography to assess regurgitant severity. This is best used to examine blood flow and has various indexes to do so; Pulsed Wave Doppler, Continuous Wave Doppler, and Color Doppler.[23] With the use of these three implications and further analytical methods, valvular regurgitation is able to be quantified.

1.3.3.1 Pulsed Doppler

Pulsed Wave Doppler (PWD) is an index used when conducting a TTE echocardiogram. Recordings of the velocity time integral (VTI) are used along with valve measurements in order to obtain the flow rate and stroke volume at the mitral annulus.[7; 23] This technique is also used to estimate the function of the LV in diastole during this time by looking at the tracings of the mitral leaflets. When severe MR is present, mitral inflow shows to have early filling due to an increase of flow across the valve during diastole.[23] This technique is best used as a qualitative indicator detecting variations in blood flow during regurgitation, as well as accompanying other techniques and quantification measures taken.[22]

1.3.3.2 Continuous Wave Doppler

Continuous Wave Doppler (CWD) best displays peak velocity of the MR jet, showing high pressure gradient of the LV/LV during systole, as well as timing of regurgitation.[9; 22] Signal density is a useful indicator of MR severity and correlates with angiographic standards, with a dense signal suggesting severe MR and a faint signal suggesting mild MR.[7; 18; 23] CWD can also gauge severity by pulmonary hypertension, volume overload in the cardiac chambers, and intensity of the signal regarding the MR jet.[7; 16] This method should also be used with other index techniques as the pattern and size / shape of the jet can differ considerably, based on the machine that is being used, settings applied, and the alignment of the transducer in regards to the regurgitant jet.[16] In eccentric MR cases, this proves to be somewhat difficult to record the full envelop of CWD, due to jet eccentricity and transducer placement.[9]

1.3.3.3 Color Doppler

Color Doppler (CD) is the most common clinical technique used, displaying the spatial distribution of velocities within the image plane that is being captured.[7; 22; 23] The direction and shape of the jet shown are beneficial in mechanism diagnostics, as an eccentric jet signifies pathologic regurgitation.[16] There is broad assumption that as the size of the jet increases, as well as the regurgitant volume into the LA, the level of severity also increases. However, this can also widely differ due to hemodynamics, ultrasonic machine / settings used, and operator technique.[9]

Though CD is considered best technique when detecting MR and its severity, a more cohesive approach is needed when attempting to quantify regurgitation severity accurately. Through Color Doppler three principle elements are able to be obtained; the origin of the regurgitant jet and the width, spatial orientation of regurgitant jet area, and the flow convergence through the regurgitant orifice.[16; 22; 23] It has been indicated in many studies that the measurements taken from these images, and that are further implemented in analytical methods, is the most accurate way to assess MR severity.[22; 23]

1.4 Quantification of Mitral Regurgitation

1.4.1 Regurgitant Jet Area

Assessing the regurgitant jet area is one approach that can be used to help determine MR severity. As a regurgitant jet indicates that MR is present, the area greatly depends on the mechanism of MR, which can often result in inaccurate measurements.[7; 23] This method is only relevant when evaluating central jets, as eccentric

jets will be severely underestimated due to the Coandal effect and being influenced by the LA wall.[16; 23] This method is also flawed by not accounting for hemodynamics, as well as being largely affected by machine settings.[16] It is imperative that this method is used along with examining the vena contracta and flow convergence.[22]

1.4.2 Vena Contracta

Measurement of the vena contracta width (VCW) is taken at the smallest high velocity sector of the jet, which is located downstream or at the regurgitant orifice.[7; 19; 23] This The width is measured in the long-axis plane perpendicular to the commissure, but can vary during systole or under the affects of other hemodynamics present.[7] VCW is typically smaller than the anatomic regurgitant orifice area due to boundary affects, representing the effective regurgitant orifice area (EROA). Unlike regurgitant orifice area, VCW is not as affected by machine parameters as it is independent of the flow rate, driving pressure, and has a high velocity.[16; 23] This method is also able to evaluate concentric and eccentric, however, there is some assumption that the regurgitant orifice is circular in shape.[9] As it is also unclear how to evaluate multiple jets present, as well as underestimating severity when the orifice is elliptic in shape, the vena contracta method should be used alongside with the flow convergence method to better assessing these cases.

1.4.3 Flow Convergence ; Proximal Isovelocity Surface Area

Evaluating the proximal isovelocity surface area (PISA), also known as flow convergence, has proven to be the preeminent approach to quantify MR severity. This method is based on the continuity equation and principle that as blood flows through the orifice the velocity increases, forming hemispheric shells of increasing velocity, with a decreasing surface area.[16; 23] Color Doppler imaging identifies the flow convergence near the regurgitant orifice area (shell). The radius of the hemispheric shell is measured, allowing for peak flow rate and EROA to be determined, assuming that the PISA radius is occurring simultaneously at peak regurgitant flow.[7] Clinicians are instructed to measure PISA radius of the hemispheric shell for these calculations, but there is minimal specifications on how to do so throughout present literature and guidelines.[12] As the radius is measured to the aliasing velocity point of the color Doppler image (known as the PISA radius), this can be highly dependent on machine parameters implemented.[12] The placement of the transducer to capture the orthogonal images can be somewhat difficult, as it needs to align with the regurgitant jet / orifice, showing that this method is most accurate for concentric jets.[7; 16; 23] However, the majority of orifices present in MR are dynamic and not circular in shape, but rather more of an ellipse.[7; 9] This can greatly affect the PISA calculation by showing errors in the formula, underestimating flow rate and EROA.[7; 16; 22] There is also an assumption that velocity distribution is symmetrically hemispheric, which is unlikely to hold true when evaluating orifices that are ellipse in shape, eccentric jets, and multiple jets present.[9] Although there is a hemielliptic formula that may be used, this mainly addresses the orifice structure. The images needed for this method have also proved to be extremely difficult to obtain,

as 3orthogonal measurements are needed. A modified version of the hemielliptic method has been proposed and shows substantial promise as to how these measurements may be more effectively taken in a clinical setting.[6]

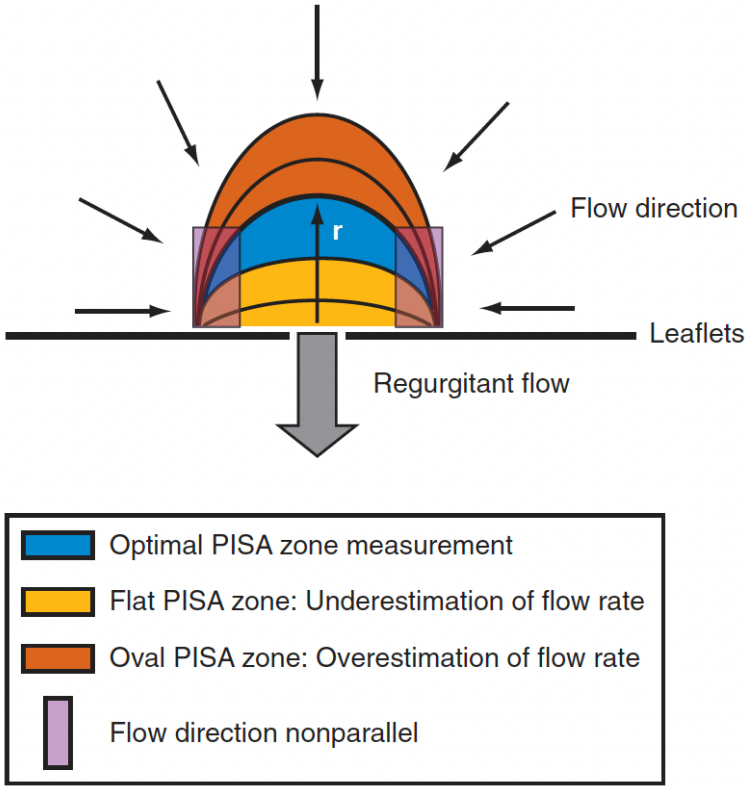

Figure 1.4.1: Proximal isovelocity surface area depiction of PISA shell. Measurement of the radius should be taken at the aliasing velocity; if not, estimation of flow rate will be inaccurate.[16]

1.5 Treatment of Mitral Valve

Surgical intervention is often needed in patients with moderate to severe MR in order to provide longevity and a better quality of life. Once an echocardiogram has been

performed, and MR severity has been determined, a cardiac surgeon will often perform a TEE (if one has not been done already) to determine whether or not the valve should be repaired or replaced.[14] Through TEE precise delineation of the valve apparatus will be evaluated prior to surgery, as well as overall hemodynamics, and potential surgical procedures will be discussed amongst the surgeon and cardiologist, before presenting the best options to the patient.[14] Although surgical repair is often needed for those suffering from severe MR, the desired method is to implement a repair technique of the valve, as it is a much less invasive procedure than that of valve replacement.

1.5.1 Surgical Valve Replacement

Mitral valve replacement is needed when the valve cannot be repaired. This is done by removing the innate valve, replacing it with a mechanical valve or a valve made from human, cow, or pig tissue. However, mechanical valves are often chosen as biological tissue valves degenerate as time goes on and will eventually need intervention of a second surgery.[14] MV replacement can be executed through a surgical procedure or through new technology using transcatheter mitral valve replacement (TMVR). Once a mechanical valve is inserted, patients will need to take anticoagulation medications for the remainder of their life. It is prominent during the replacement process that chordae is preserved as much as possible. There are currently 8 TMVR devices in preliminary trials, majority of which having a transseptal approach to implementation.[5] Though replacement of the valve post-operation has a high success rate, some difficulties due to this are long recovery times and medical complications that may occur during operation

time. For these reasons, repair of the valve is most sought after, especially with new technologies that are being able to do so.

1.5.2 Surgical Valve Repair

MV repair is the most sought-after option in addressing MR, as a minimally invasive procedure that is able to repair valve leaflets, chords, or by removing misplaced tissue. Repair is done through using edge-to-edge leaflet coaptation with a clip securing anterior and posterior leaflets where the regurgitant orifice is located.[13] Advantages of repair is evasion of long-term anticoagulation's, minimal recovery time, low risk of medical complications, and, most importantly, preservation of the continuity between the mitral annulus and the papillary muscle. This preservation is crucial as it correlates with the decrease in operation mortality.[14] Through transcatheter mitral valve repair, the technique of implementing a device is being used by cardiologists as a means of restoration for those with moderate to severe MR. The MitraClip device is currently the only FDA approved device for repair via implantation through a transcatheter approach. Currently, implementing a MitraClip in patients affected by primary MR is not often executed, as viability and surgeon experience need to be accounted for.[13]

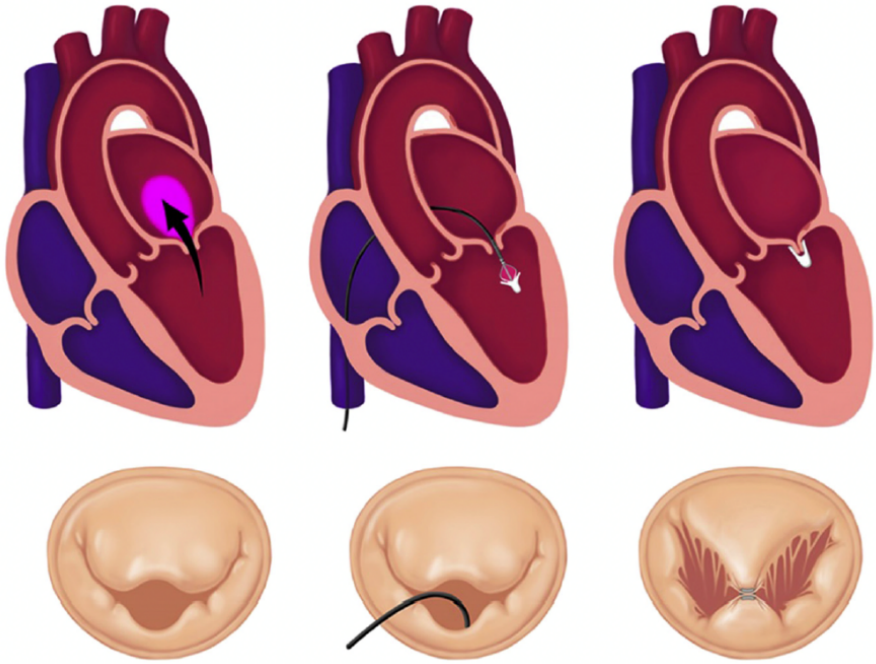

Figure 1.5.1: Mitral valve before and after MitraClip implantation. Double orifice present post-operation.[2]

1.5.2.1 MitraClip Implantation

The MitraClip is a new technology and has quickly become the gold standard treatment option for those affected by MR. It is minimally invasive procedure, able to be placed in the heart via transcatheter. The clip system is made up of two parts; a steerable guide catheter and the clip delivery system. The clip itself is polyester-covered cobalt chromium with two are "arm" that are controlled by the delivery system during implantation. The inner portion of the clip are two grippers that help to secure the leaflets as the clip closes. The tissue is then firmly secured through the arms of the clip and grippers. Once there is reduction in backflow, showing minimal regurgitation, the clip is locked into place.[2] The device essentially uses the edge-to-edge principle. This is a

surgical technique that was introduced by Ottavio Alfieri in the 1990's, suturing the leaflets at the site of regurgitation. A centrally applied suture resulted in a double orifice repair, where as a suture applied to either side of the orifice resulted in one opening, referred to as a commissural repair.[2] MitraClip procedure has proven effective in reducing regurgitant volume and improving clinical symptoms. At present, those with secondary MR are predominantly selected for MitraClip procedure. Though it has also been used for cases regarding primary MR, as it is still a new technology, the effects and outcomes due to clipping may vary based on patient-specific heart anatomy and etiology.[17]

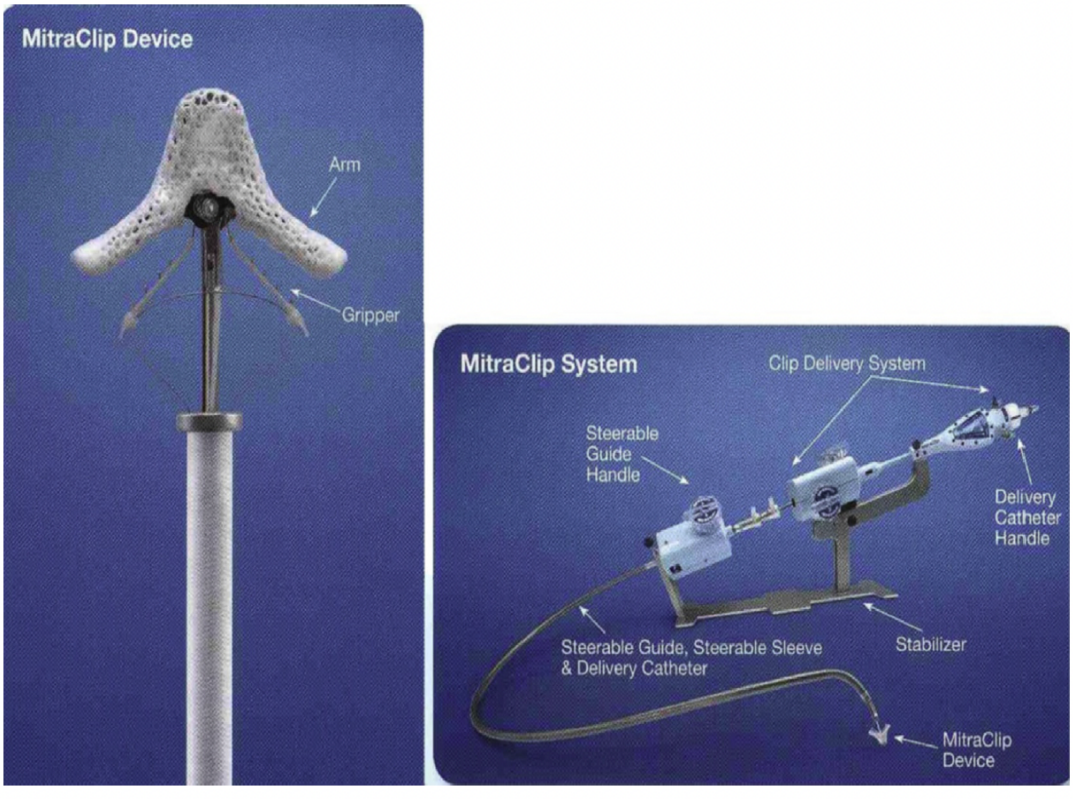

Figure 1.5.2: MitraClip device system.[2]

1.6 Simulated Cardiovascular Biomechanics

With many clinical applications available to quantify MR severity, a significant flaw is the absence of consistent technical procedures and a gold standard used to do so.[11] As the ASE has recommended that the most accurate way to quantify is through the PISA method, machine parameters administered and clinician techniques can affect severity quantification by both under and over estimation.[11] Through the use of finite element (FE), fluid-structure interaction (FSI), and computational fluid dynamics (CFD), various simulations have been performed emulating echocardiography and evaluating MR through models constructed from patient-specific CT data. Though some studies have shown to be inconclusive, the development of CFD aims to prove its importance in medical headway. The ability to use patient-specific data can be used in numerous ways; simulating plausible treatment methods, evaluating efficacy, and predicting possible complications.[3]

1.7 Cardiac Simulators and Ex vivo Testing

As clinical techniques, analytical models, medical devices, and computational methods continue to develop, it is essential that these new practices be assessed and perfected before executing in a clinical setting. In the past, cardiologists and cardiac surgeons have learned new device implantation through low-fidelity simulations, giving little to no visual control and unfeasible physiologic conditions.[10] As medical devices and surgical procedures continued to evolve, so did the need for a simulator emulating biological conditions. There are currently a few simulators that use biological organs, in order to emulate anatomic and hemodynamic cardiac circumstances. These simulators

allow for practice to be done in the Cartesian X,Y and Z planes, as well as being able to monitor and regulate hemodynamic conditions in a controlled environment.[10] Ex vivo testing with the use of biological simulators proven to have a vast impact on clinical practices through validating, optimizing, and designing new techniques used.[15; 21] Most simulators use porcine myocardium as human analog because of similarity in anatomy, size, and tissue microstructure.[8]

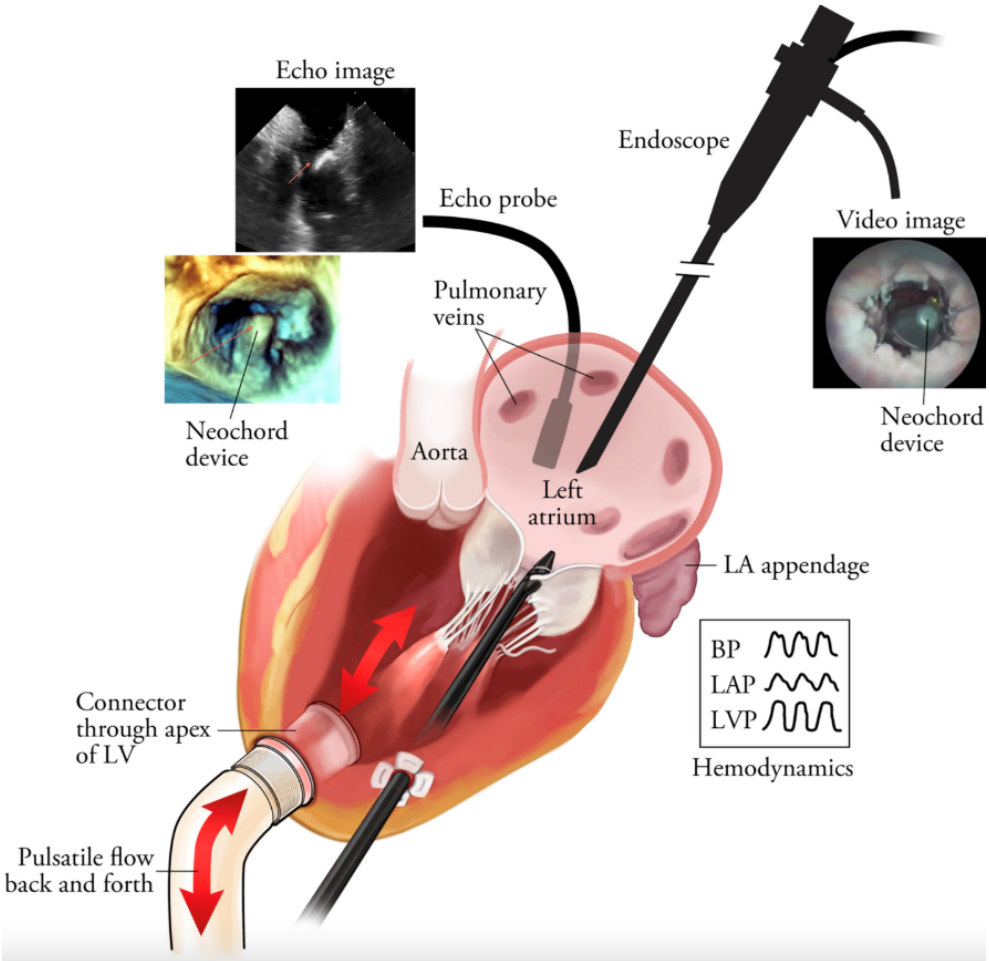

Figure 1.7.1: Representation of left-heart simulator while undergoing artificial chordae replacement.[10]

1.8 Research Aims

As there is no single or correct answer for a pathway to therapy, it is crucial to have an experienced and multidisciplinary cardiac team. It is currently recommended that those with chronic primary MR undergo surgery, however, MitraClip is now being considered as a plausible option. It has shown to be safe and effective in reducing regurgitation, LV remodeling, and clinical symptoms. This therapy needs to be further explored as it may be the leading choice for the aging population affected by primary MR.[13; 20] However, studies have shown that in modern clinical practice less than half of patients that have moderate to severe MR receive adequate treatment, mainly due to not being properly addressed by the treating physician.[20] This goes to show the importance of recognizing MR severity accurately and need to optimize practices, as well as modify current guidelines.

As previously shown, there are an array of difficulties and limitations in current practices seeking to quantify severity as accurately as possible. This paper aims to give a comprehensive engineering analysis of quantification using the modified-hemielliptic PISA method, impact of the MitraClip implementation, ex vivo testing methods, and further development of a biological simulator. More specifically, through the use of computational fluid dynamics, the modified-hemiellptic PISA method will be used to quantify severity in native valves of mild, moderate, and severe MR, as well as valves with MitraClip implantation showing mild, moderate, and severe. These cases are classified as primary MR with orifices that are ellipse in shape and have eccentric regurgitant jets. This practice will then be attempted through ex vivo testing, as well as originating the first full cardiac simulator. Comparing the regurgitant flow rates found

using the modified PISA method to the actual flow rates found in the computational simulations will display the relevance of using CFD in a clinical setting. Furthermore, it will give insight as to how clinical techniques in quantifying MR may be improved.

Chapter Two: Methods

2.1 Ex vivo Testing

Two experimental testing systems were designed to perform ex vivo testing; a steady flow and a pulsatile flow system. Both flow systems had advantages and disadvantages throughout testing, however both proved to be highly beneficial in intracardiac visualization, displaying the importance of hemodynamics, and significance of clinical practice assessment. Each simulator was used to implement doppler echocardiography procedures on porcine heart subjects and gather necessary data to evaluate quantification of MR severity. A working solution of 37% glycerin in saline was used as the properties emulate that of blood. Prior to each testing trial with both simulators, flow meter calibration was performed.

2.1.1 Steady Flow Design

Experimental testing was first executed using a steady flow system. As a means of preliminary testing, this methodology allowed for evaluation of pitfalls within a simple flow system connected to a porcine heart, as well as indicating potential pitfalls within a pulsatile flow system. This system was affixed to the left side of the heart only, through the aorta and pulmonary veins, and was done so using tubing adapters and clamps. Connection of the pump was also implemented at the left ventricle with an array of 3D printed adapters that were designed, CAD modeled, and printed “in house" by

a Formlabs 2 resin printer, to ensure a secure connection with minimal leakage. The flow system had a control valve, Transonic flow meter, and was driven by an Iwaki Magnet Pump. Once all connections were in place and secured, the working fluid was applied. As testing trials progressed, many techniques were investigated to find optimal results.

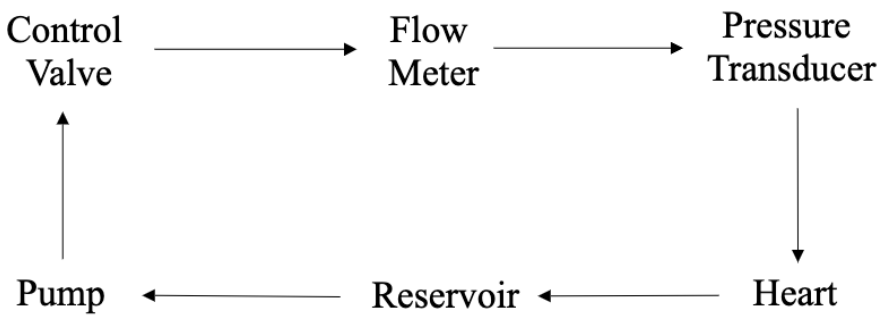

Figure 2.1.1.1: Schematic of Steady Flow System.

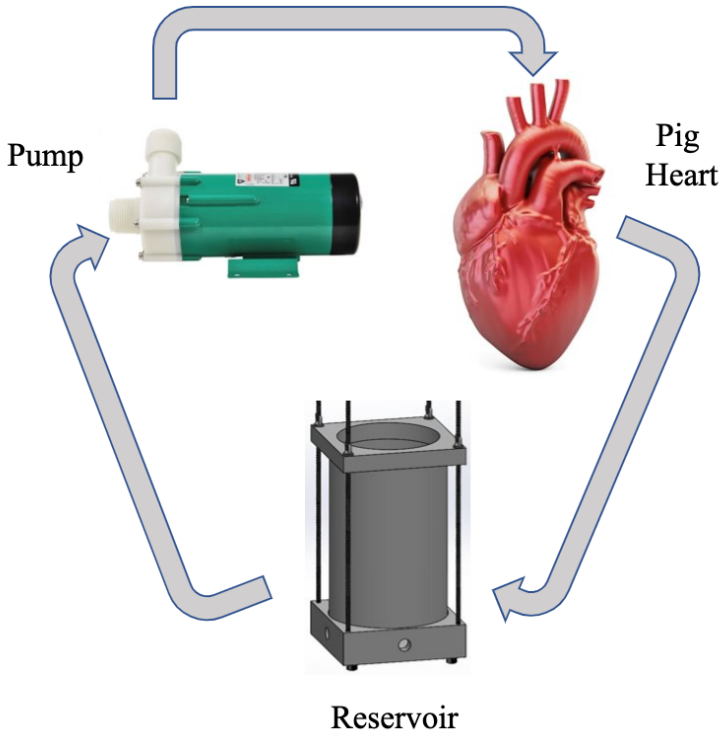

Figure 2.1.1.2: Steady Flow System design.

2.1.2 Pulsatile Flow Design

A steady flow system is adequate for initial testing methods, however the need for a pulsatile flow system in order to initiate physiologic attributes is of significance. Furthermore, the need for a full cardiac simulator, as opposed to a sole left heart simulator, is necessary in order to give full hemodynamic properties throughout the cardiac cycle. As previously only left heart simulators have been created and used in cardiac ex vivo testing, these systems were evaluated and assessed prior to designing a full cardiac simulator.

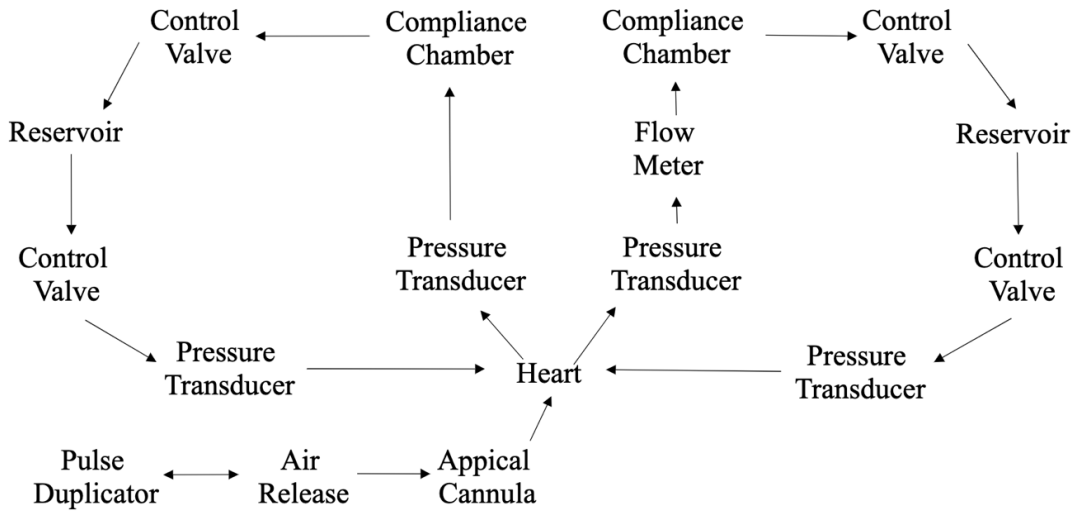

Figure 2.1.2.1: Schematic of Full Cardiac Simulator (i.e. Pulsatile Flow System).

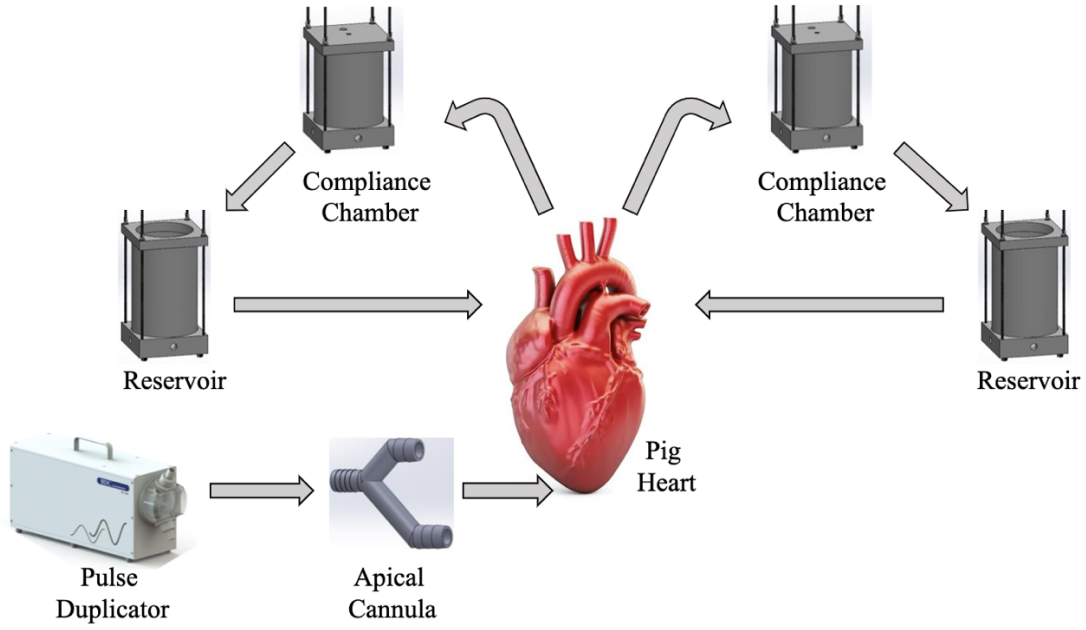

Figure 2.1.2.2: Full Cardiac Simulator design.

2.1.3 Full Cardiac Simulator Construction

Compliance and reservoir chambers needed for the system were designed after BDC Laboratories models that are currently sold on the market. CAD models based on these designs were created in SolidWorks, with some modifications in measurements to fit other necessary supporting parts. Large pieces of acrylic were obtained from Colorado Plastics Company and modified / cut by a HAAS Super Mini Mill computer numerical control (CNC) machine. Once the chambers were assembled, they were fit to the standard ¾ inch tubing used throughout the system. As shown in the schematic, each compliance chamber was connected to a control valve, reservoir, and pressure transducers at the valves. Both pressure at the valves and flow rate were monitored throughout testing. All pieces were affixed by appropriate tubing adapters and

clamps ensuring minimal leakage. The compliance chambers were connected to the heart at the superior vena cava and the aorta (with a flow meter inserted between this connection), and with the reservoirs connected to the pulmonary artery and pulmonary veins. BDC Laboratories PD-1100 Pulsatile Pump System was attached to the heart at the apex, with insertion into both the right and left ventricle. This was done by an array of 3D printed cannulas that were tested for optimal connection. As the pulsatile pump pistons run optimally with water, a feedback loop was implemented to ensure minimal working solution to interfere with the pump, as well as having a control outlet for air trapped within the system. Once the system was attached to the heart and all clamps were secured, the working fluid was applied. The system was run a few times prior to testing to inspect for any leakage or air within the system present.

2.2 Experimental Subjects

As porcine hearts remain to be an appropriate human analog, they were chosen to be used as the experimental subjects throughout this study. The first set of subjects were obtained through Biology Products, specializing in specimens used for academic purposes. The second set of subjects were obtained through a local slaughterhouse. As the first set of hearts were withdrawn from the pericardium upon receiving them, the second set of hearts were attached to the lungs and pericardium. This was removed carefully, ensuring to leave as much of the superior vena cava, aorta, pulmonary artery, and pulmonary veins as possible to assure secure attachment to the flow systems. Measurements of heart connection points were often taken, however the size showed to vary minimally. Prior to testing, all hearts were

thoroughly rinsed of blood and cleaned of unnecessary remaining pieces. Each test heart was then manipulated in various ways throughout the testing trials to emulate MR pathophysiology. This was done first by removing the aortic valve entirely, pressurizing the heart through the aorta, and inflating the mitral leaflets. Cuts were then made on the leaflets as close to the commissure as possible, either on the anterior leaflet or posterior leaflet. The removal of some chordae tendineae was also occasionally applied. Once the valve was modified, the heart was inspected for any present cuts, placing sutures on any visible to mitigate leakage.

2.3 Doppler Echocardiography Techniques

There are currently parameter guidelines implemented throughout clinical practice to obtain the necessary images to quantify MR through PISA, however, machine settings and clinician techniques may vary, causing measurements to be less accurate. While these guidelines have been proven to be pertinent to concentric jets with an orifice being of circular shape, they remain to be scrutinized when it comes to eccentric jets and orifices that are elliptic or organic in shape.[22] The shape of the regurgitant orifice, affecting the shape of the regurgitant jet and therefore vital transducer alignment, is what remains to complicate accuracy of all PISA calculations.

2.3.1 Mitral Regurgitation Parameters / MR TTE methods

Transthoracic echocardiogram was performed on heart subjects using a Philips iE33 Ultrasound Machine and x-51 transducer. Methodology and guidelines proven effective throughout clinical practices of MR quantification were executed. A certain

series of images for necessary measurements need to be taken for MR quantification. The apical four chamber view is used for an optimal visual of all four heart chambers, with the parasternal long and short axis view used for more complex pathophysiological affected valves, namely when eccentric jets are present.[9] Proper alignment of the transducer with the present jet is essential, as inaccurate data can be acquired if not, leading to inaccurate severity diagnosis.[23]

Certain technical parameters need to be accounted for on regards to optimal acquisition, in order to enhance visualization of the MR orifice area by the PISA shell. These settings were first checked making sure color Doppler variance mapping was shut off prior to testing.[19; 23] The mitral regurgitant jet is often referred to as the mosaic color protruding from the mitral valve into LA during systole. Images are taken throughout systole to examine the proximal flow convergence region (PFCR) where the isovelocity shell is seen, with the most accurate PISA measurement typically taken mid-systole. As radius is measured to the aliasing velocity (I.e. the blue-red interface) and is affected by the compilation of these parameters, it is crucial that optimization is be accurate as possible. Color gain was considered lowered as random color noise can cause inaccurate visualization of the jet. The Nyquist limit defines frequency and is considered to be the most important factor when taking measurements for PISA, as it most directly affects the resolution and integrity of the PISA shell.[16] This was considered within the range of 40-60 cm/second.[9; 16; 19] Within this range has shown to give the optimal imaging of the PISA shell, however it may still be somewhat unclear as to where aliasing velocity is and where radial measurement should be taken. In order to account for this, a practice of baseline shifting is applied. This is done by shifting

the color scale baseline 30-40 cm/second in the direction of the regurgitant jet.[9; 16; 19; 22] After necessary images were taken for PISA measurements in the orthogonal views, continuous wave Doppler measurements were taken to obtain the peak velocity of MR. Referred to as "color compare / suppress" color Doppler was switched on and off with CW Doppler to take a series of images. This method is known to improve accuracy in identifying both PISA shell and peak velocity.[19] As peak velocity is often found around 5 m/second, this was used as a gauge.[19; 22]

Ultrasonic gel was applied to the transducer prior to placement on the heart. The mitral valve was located using 2D Doppler setting, as this is the best image depicting the anatomy. The color Doppler and CW Doppler techniques were then implemented. Throughout testing, the transducer was placed on various parts of the heart, in means of obtaining the most accurate measurement with the jet (s) present within the test subject. As heart subjects were manipulated in various ways emulating MR, transducer placement aimed to align with the present jets as accurately as possible. Various approaches were used to obtain this (see appendix), however, the typical apical and parasternal views were utilized the most. This procedure was practiced with both the steady and pulsatile (full cardiac simulator) flow systems. The technical acquisition techniques described for MR quantification via TTE above were used throughout experimental testing.

2.4 Computational Fluid Dynamics

2.4.1 Model

Multiple computational models of the left heart (I.e. the left atrium, mitral valve, and ventricle) were created to test MR simulations. The left atrium and ventricle were based on de-identified patient-specific CTA data acquired from the University of Utah.

The mitral valve geometries were created based on a previous research study (et al. Delgado, V., Tops, L. F., Schuijf, J. D.). In this study patients underwent a multi-splice spiral computed tomography (MSCT) scanner, acquiring 64-slices, as well as an electrocardiogram simultaneously recording data throughout multiple cardiac cycles for appropriate reconstruction.[4] Patients assessed in this study had heart failure and were affected by moderate to severe MR. Data showed asymmetric deformations of the mitral valve, especially in regard to the angles of the posterior leaflet values at the central and posteromedial levels, resulting in notably higher differences of MV tenting height at these levels.[4] A "base" mitral valve CAD model using SolidWorks was created based on this data with the annulus of the valve constructed to fit the previously obtained LA and LV model used. This valve was further modified to emulate mitral regurgitant valves and mitral regurgitant valves with MitraClip implementation. As the shape of the commissure is a product of the tenting heights in place, insertion of elliptical orifices at the commissure showed to be in applicable position that would display eccentric regurgitant jets. The bottom of the left ventricle was removed, as this would be the flow inlet.

Table 2.4.1.1: Details of Native Mitral Valve orifices created.

Case	Short Axis Radius, mm	Long Axis Radius, mm	Calculated Orifice Area, mm^2	Actual Orifice Area, mm^2
NMV Mild	0.85	1.69	4.51	5.00
NMV Moderate	1.29	2.59	10.52	11.72
NMV Severe	1.78	3.55	19.80	22.13

2.4.1.1 Native Mitral Regurgitation Valve

A total of three cases of native mitral regurgitant valves were modeled. This was done by cutting an ellipse orifice through the model at the center of the commissure. Three orifice sizes were chosen to emulate mild, moderate, and severe regurgitation. These models were then further tested through the simulation process.

Table 2.4.1.2: Details of MitraClip Mitral Valve orifices created.

Case	Short Axis Radius, mm	Long Axis Radius, mm	Calculated Orifice Area Total, mm^2	Actual Orifice Area Total, mm^2
MCMV Mild	3.39	6.77	4.70	5.09
MCMV Moderate	4.38	8.75	12.88	14.51
MCMV Severe	5.18	10.35	21.74	24.95

2.4.1.2 MitraClip Implantation in Mitral Regurgitation Valve

The native mitral regurgitant valves with ellipse orifices corresponding to mild, moderate, and severe MR were further modified by mimicking MitraClip implantation. This was done by using the dimension of the width of the MitraClip, 5mm, a method also

previously used in CFD / FSI studies.[3] With the clip in place at the center of the previous regurgitant orifice, each valve then had two smaller ellipse orifices remaining on both sides of the clip.

2.4.2 Mesh

After six complete models were assembled (i.e. atrium, ventricle, and respective valve) and displayed no gaps within geometry connection points, meshes were created based on each model. This was done using the fluid focalized software Pointwise. Four meshes were initially made of the native mild MVR model in order to assess mesh quality. The element size of the valve geometry remained the same throughout the four complete model meshes, however the element size of the left atrium and ventricle were modified, evaluating different element sizes. Meshing of different element sizes and further testing these models through the fluid simulation allows for the comparison of convergence. The mesh that contains the least amount of elements and fully converges is then chosen as this certifies optimal computational run time while supporting a high-fidelity simulation. The mesh element size of the LA / LV referred to as Medium Fine was chosen to be used throughout the 6 models. Prior to fluid simulation testing, each mesh quality and accuracy was assessed, validating that no errors were present.

2.4.3 ANSYS Fluent Simulation

Fluid simulations were run by ANSYS Fluent software. As shown during the mesh convergence verification process, simulations showed full convergence after 400 iterations. Prior to running the fluid simulation, all boundary

conditions parameters were evaluated and set. These boundary conditions were applied to all six model simulations. Once all fluid simulations were completed, all data was exported to be further processed.

2.4.4 Simulated Echocardiography

As each CAD model created had an ellipse orifice, the hemielliptic PISA model would be implemented to quantify for regurgitant severity. The original hemielliptic PISA model is calculated by obtaining three measurements through 3 orthogonal views; 1) the radius in the lateral view of the long-axis, 2) the radius in the lateral view of the short-axis, 3) the radius vertical to the orifice plane.

However, due to clinical limitations of obtaining an accurate image for the approach of the vertical radius over the orifice plane, a new modified hemielliptic model has been developed. This is done by obtaining two radial measurements; 1) the radius parallel to the long-axis of the ellipse orifice, and 2) the radius parallel to the short-axis of the ellipse orifice. These measurements are able to be taken accurately in a clinical setting in the apical view.

Using Tecplot post-processing software, the fluid model was able to be manipulated in countless amounts of ways. Each of the necessary image were able to be obtained by inserting a plane directly intersecting through all mid-points of each orifice, in order to find the regurgitant jet. Further post-processing was conducted to emulate clinical factors of the Doppler Color scale and Nyquist baseline shift method, in order to take accurate measurements of the PISA shell present.

2.5 Quantification of MR Severity; Modified-Hemielliptic PISA Method

PISA measurements are taken (in clinical examination by TTE) by shifting the baseline color toward the direction of the MR jet in order to find a clear image of the PISA shell at peak regurgitation. The radius is measured from the center of the orifice, in the both the short-view and long-view, to the aliasing velocity. Hemispheric PISA is calculated as

$$PISA = 2\pi r^2 * VA \qquad \text{Equation 1}$$

2pi being the hemispheric area, r being the PISA radius, and VA being the aliasing velocity. If the base of the PISA sphere is not a flat surface, then there is a need for correction to account for wall constraint. An additional measurement is then taken of the shell angle and the equation is multiplied by the angle ratio of the walls adjacent to the orifice and 180 degrees.[7]

$$PISA = 2\pi r^2 * VA * \left(\frac{PISA\ Shell\ Angle}{180}\right) \qquad \text{Equation 2}$$

As each CAD model created had an ellipse orifice, the hemielliptic PISA model would be implemented to quantify for regurgitant severity. The original hemielliptic PISA model is calculated by obtaining three measurements through 3 orthogonal views; 1) the radius in the lateral view of the long-axis, 2) the radius in the lateral view of the short-axis, 3) the radius vertical to the orifice plane.

However, due to clinical limitations of obtaining an accurate image for the approach of the vertical radius over the orifice plane, a new modified hemielliptic model has been developed. This is done by obtaining two radial measurements; 1) the radius parallel to the long-axis of the ellipse orifice, and 2) the radius parallel to the short-axis of the ellipse orifice. These measurements are able to be taken accurately in a clinical setting in the apical view. This modified hemielliptic model can then be calculated by

$$PISA = 2\pi \left[\frac{ab^{1.6}+ac^{1.6}+bc^{1.6}}{3}\right] * VA * ((PISA\ Shell\ Angle)/180)$$

Equation 3

a being the radius of the short-axis of the orifice, b being the radius of the long-axis of the orifice, c being the PISA radius measured in the short-view or long-view, and VA being the aliasing velocity. Effective regurgitant orifice area (EROA) and regurgitant volume (RVol) are then able to be calculated flow rate measurements, quantifying regurgitation.

Chapter Three: Results

3.1 Experimental Testing

Notations were taken throughout experimental testing trials to evaluate techniques used in ex vivo testing. This was done by continuously evaluating the techniques implemented regarding the flow system, connection of the heart within the flow system, heart anatomy, and ultrasound techniques to measure regurgitation.

Figure 3.1.4 displays the Steady Flow System built for the first half of experimental testing, with Table 3.1.1 displaying the optimal techniques found regarding this system. Figure 3.1.11 displays the Full Cardiac Simulator that was built for a pulsatile flow, with Table 3.1.2 displaying the optimal techniques found regarding this design. Testing notes throughout individual trials can be found in the appendix (as shown in Table 5.2).

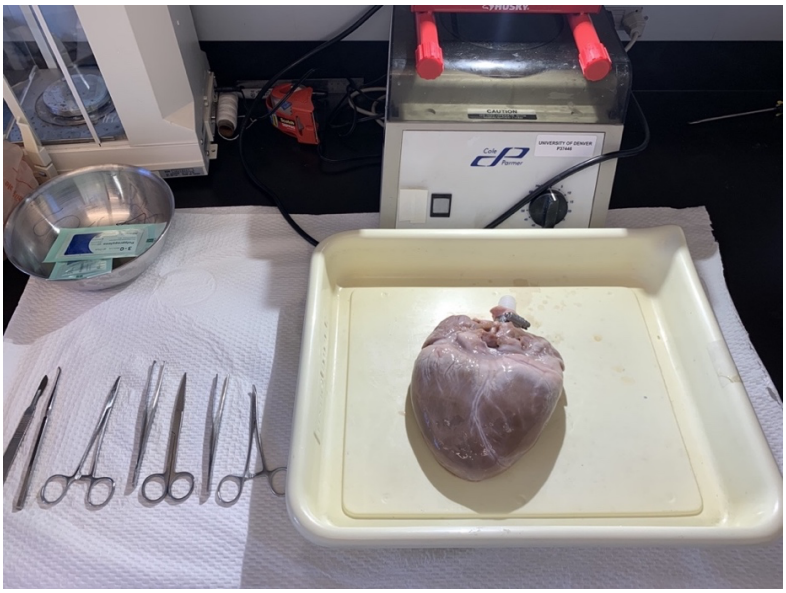

Figure 3.1.1: Preparation of pig heart. Evaluation of present cuts prior to inserting necessary sutures.

Figure 3.1.2: Mitral valve with large cuts made on A2 and P2. Suture put in place to imitate MitraClip implantation.

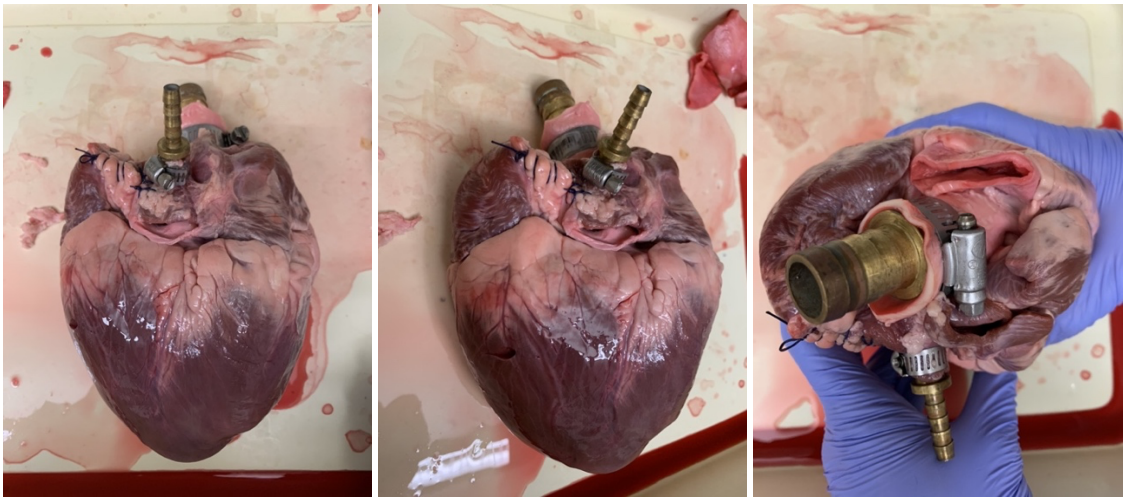

Figure 3.1.3: Fully prepared heart prior to attachment to the flow system.

Figure 3.1.4: Ex vivo Steady Flow System.

Figure 3.1.5: Heart connected to Steady Flow System. Left atrium is unattached from tubing of the system and propped up, ensuring that the LV and LA are continuously filled with fluid, with no air trapped inside.

Figure 3.1.6: Optimal positioning of the transducer on the apex of the heart. Removal of the RV in the first image showed to be the most optimal ex vivo testing method when taking necessary images / measurements for PISA.

Table 3.1.1: Steady Flow System optimal experimental testing techniques.

Flow System	• Secure connection needed of tubing to valves • Use of PIV particles is not necessary; causes unclear imaging
Heart Anatomy	• Pressurize heart before cutting the mitral valve • Cut mitral valve close to the commissure on A2 and P2 for regurgitation • Fill RV with water and insert cap • Remove RV entirely
Heart Connection	• Pulmonary veins do not need to be connected to tubing; ensure no air is caught within the LV
Ultrasound Techniques	• Find 2D image of anatomy prior to color Doppler • Shift Nyquist based on flow

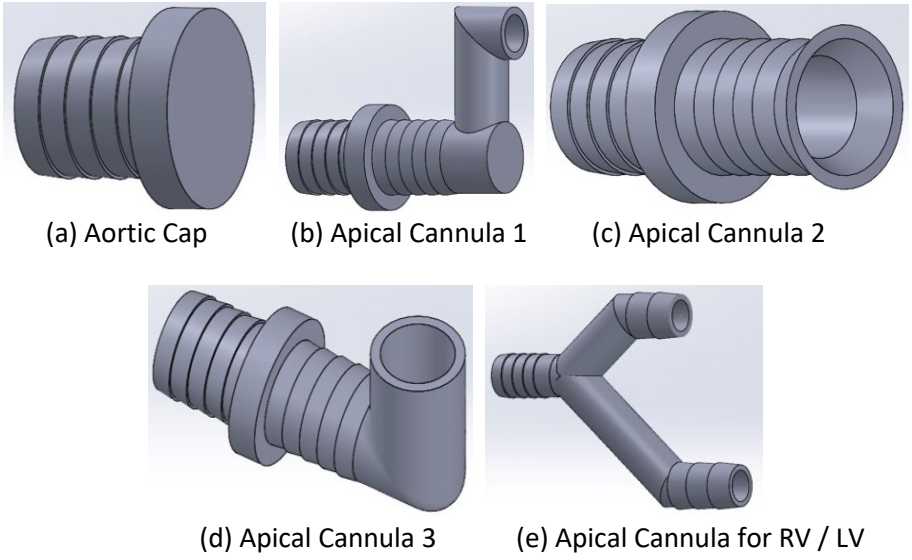

Figure 3.1.7: CAD model designs of 3D printed cannulas used throughout ex vivo testing.

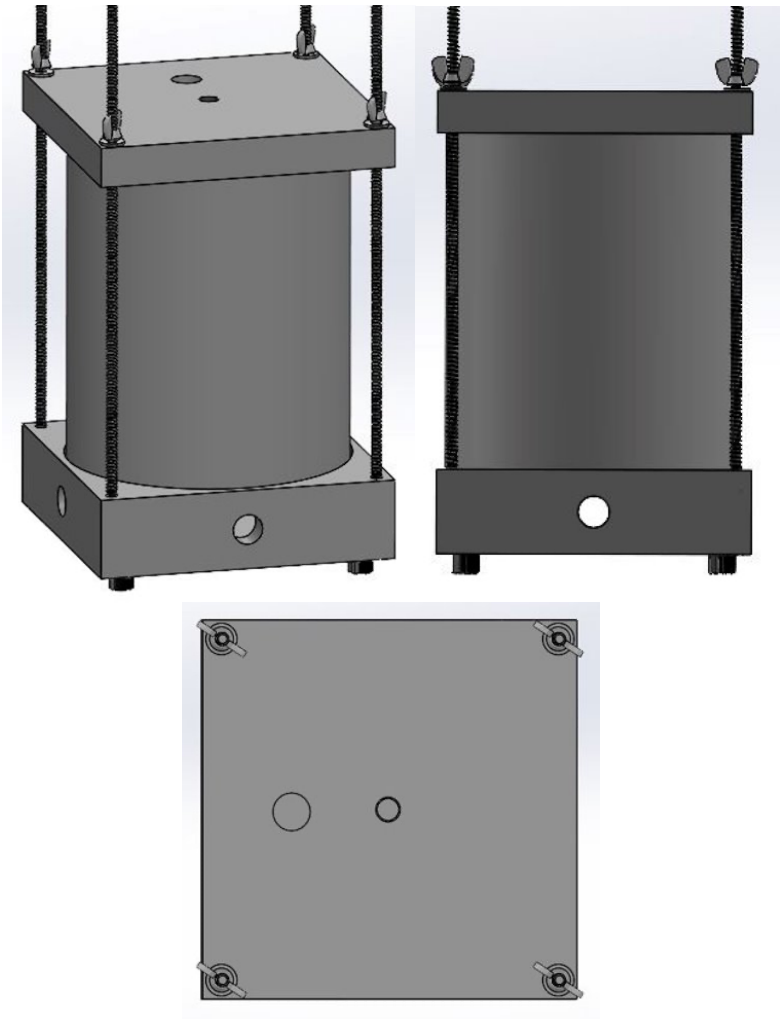

Figure 3.1.8: CAD model of Compliance Chamber made for the Full Cardiac Simulator.

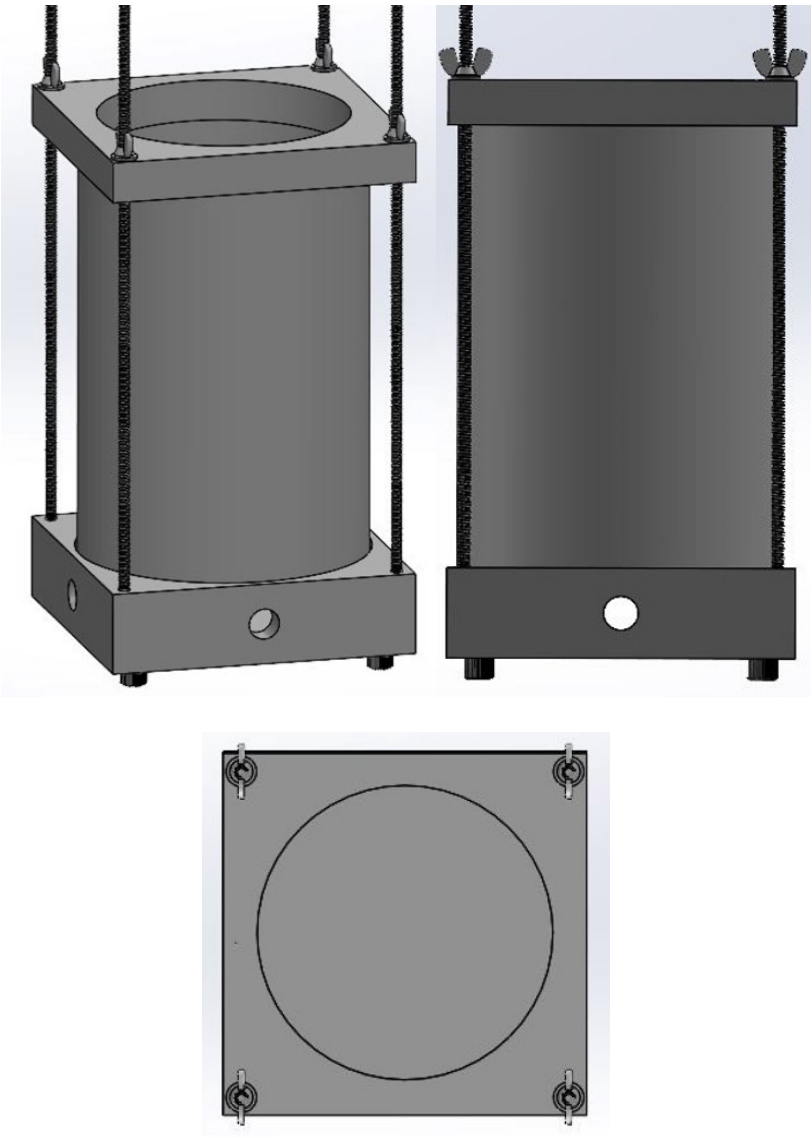

Figure 3.1.9: CAD model of Reservoir made for the Full Cardiac Simulator.

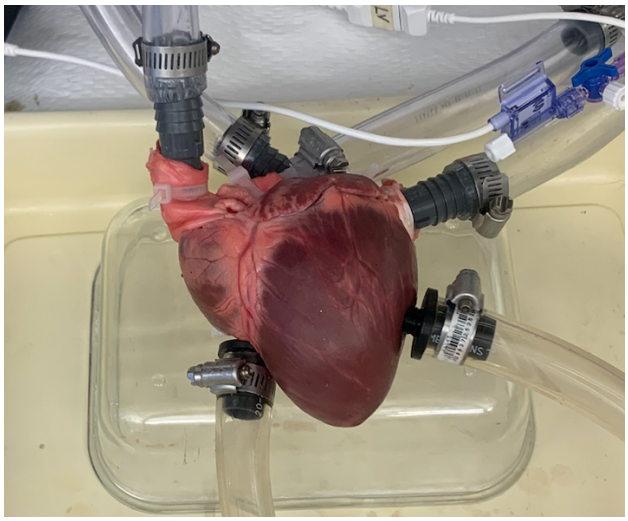

Figure 3.1.10: Test heart completely connected to the Full Cardiac Simulator at all six junction points.

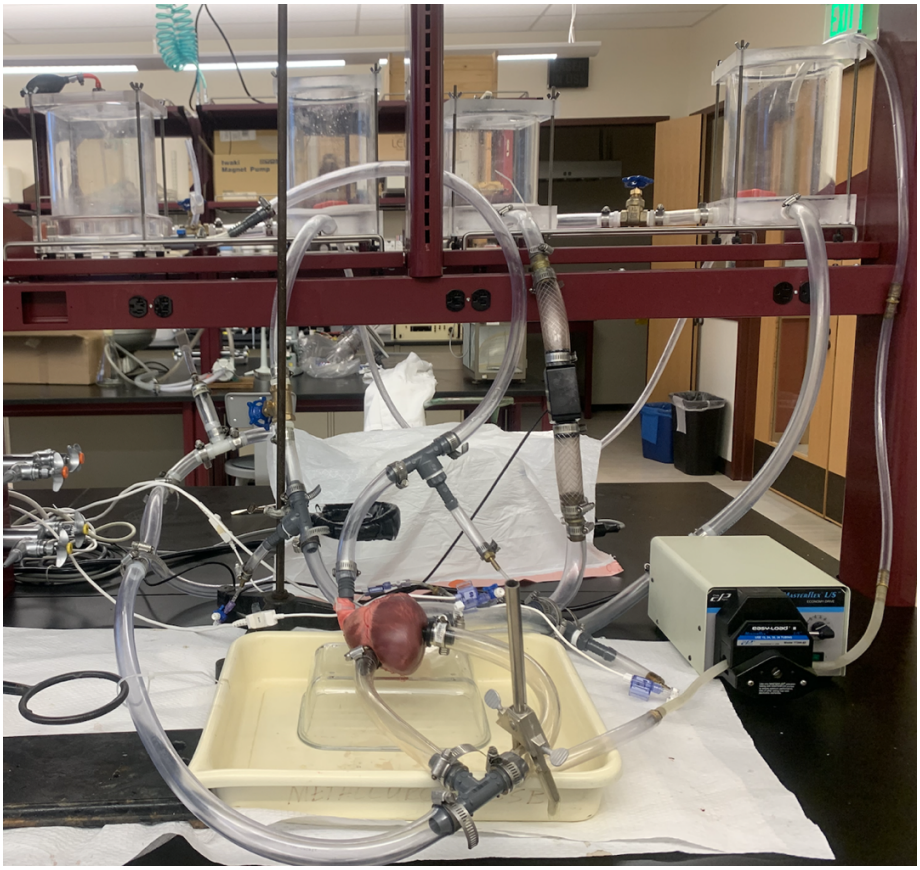

Figure 3.1.11: Ex vivo Pulsatile Flow System; Full Cardiac Simulator.

Table 3.1.2: Full Cardiac Simulator optimal experimental testing techniques.

Flow System	• Secure connection needed at all connection points ; no air within the system
Heart Anatomy	• Need to leave as much muscle at connection points as possible • Pressurize heart before cutting the mitral valve • Cut mitral valve close to the commissure on A2 and P2 for regurgitation prior to connection
Heart Connection	• All connection points must be secure; minimal to no leakage • Specialized cannula needed for apical connection point
Ultrasound Techniques	• Find 2D image of anatomy prior to color Doppler • Shift Nyquist based on flow

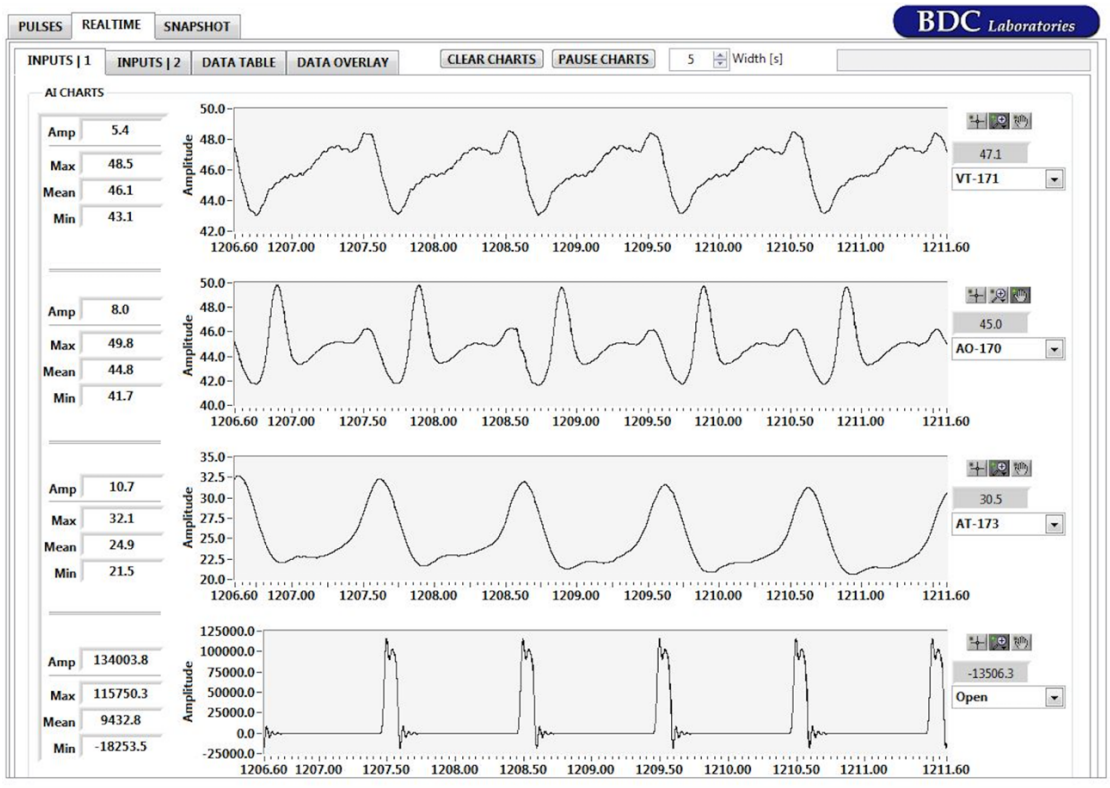

Figure 3.1.12: Pressure measurements were monitored throughout testing at the superior vena cava, pulmonary artery, aorta, and pulmonary veins via pressure transducers.

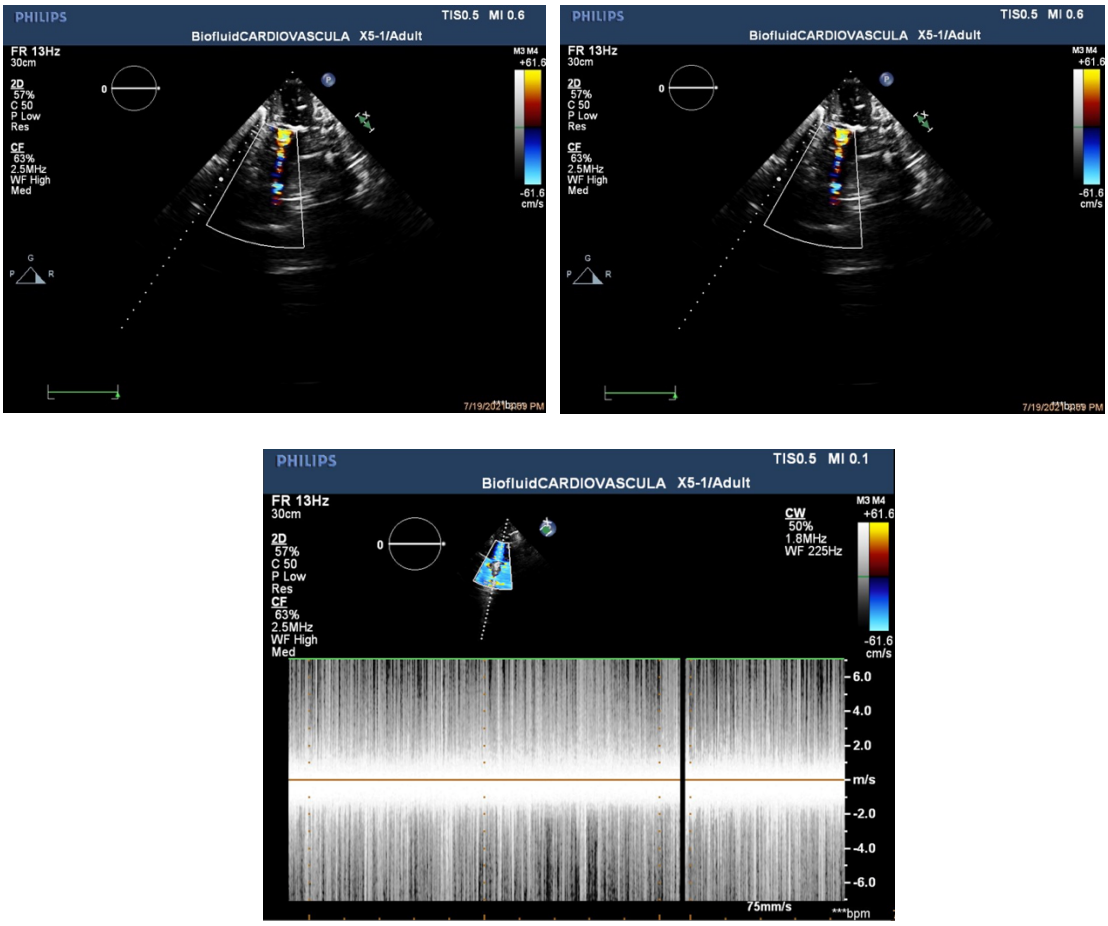

Figure 3.1.13: DICOM ultrasound imaging. Color Doppler showing regurgitant jet in the mitral valve in images 1 and 2 (top). Continuous Wave Doppler shows steady flow withing the Steady Flow System in image 3 (bottom).

3.2 Computational Fluid Dynamics ; Simulation Contours

A total of six simulations were run; three for Native Mitral Valve MR regarding mild, moderate and severe severity and three for MitraClip implantation Mitral Valve regarding mild, moderate, and severe severity. All simulations were conducted under the same conditions. The following contours show the present regurgitant jet and where the PISA radius was measured regarding the case and view of the valve. Regarding each

specific orifice of each case, two planes were created in the short-view and long-view, aligned with the anatomic coordinates. This ensured that the measurements were taken in the essential plane regarding the inflow at the bottom of the LV, as every orifice is ellipse and eccentric.

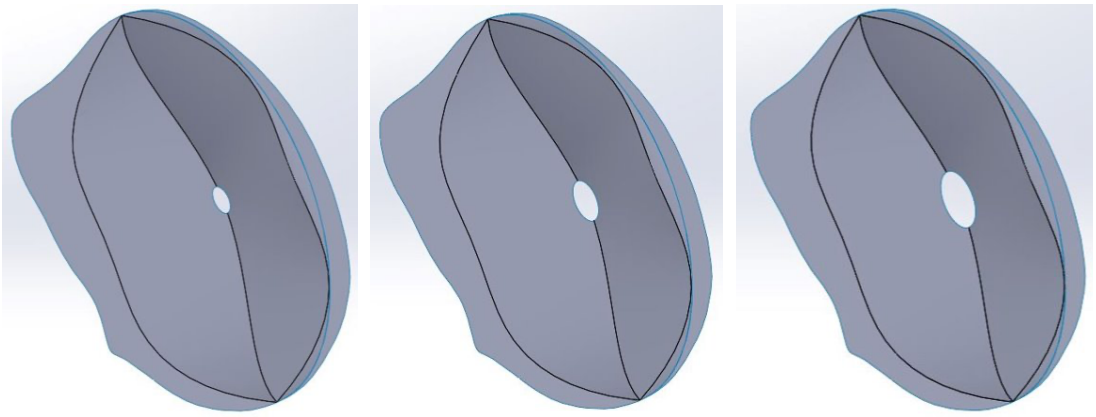

Figure 3.2.1: CAD model of Native Mitral Valves, mild, moderate, and severe, respectively.

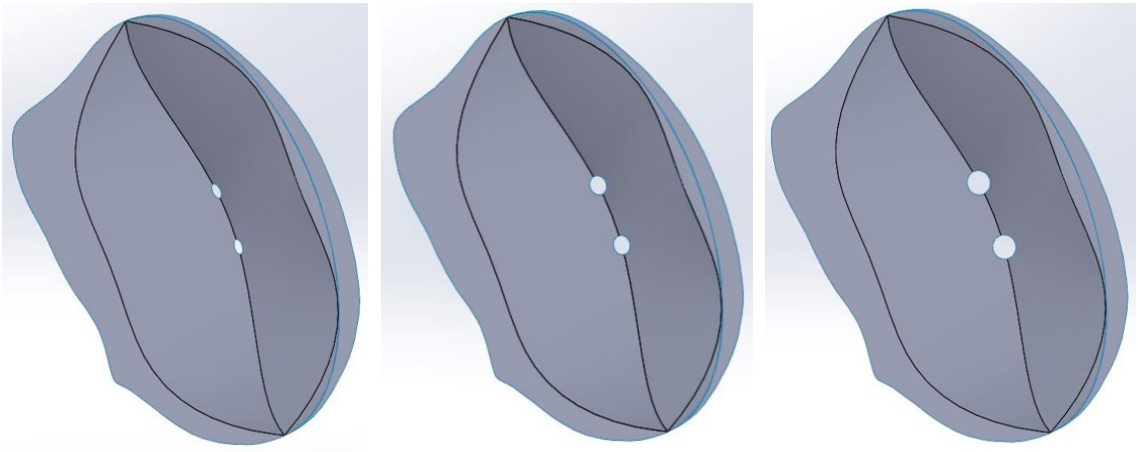

Figure 3.2.2: CAD model of MitraClip Mitral Valves, mild, moderate, and severe, respectively.

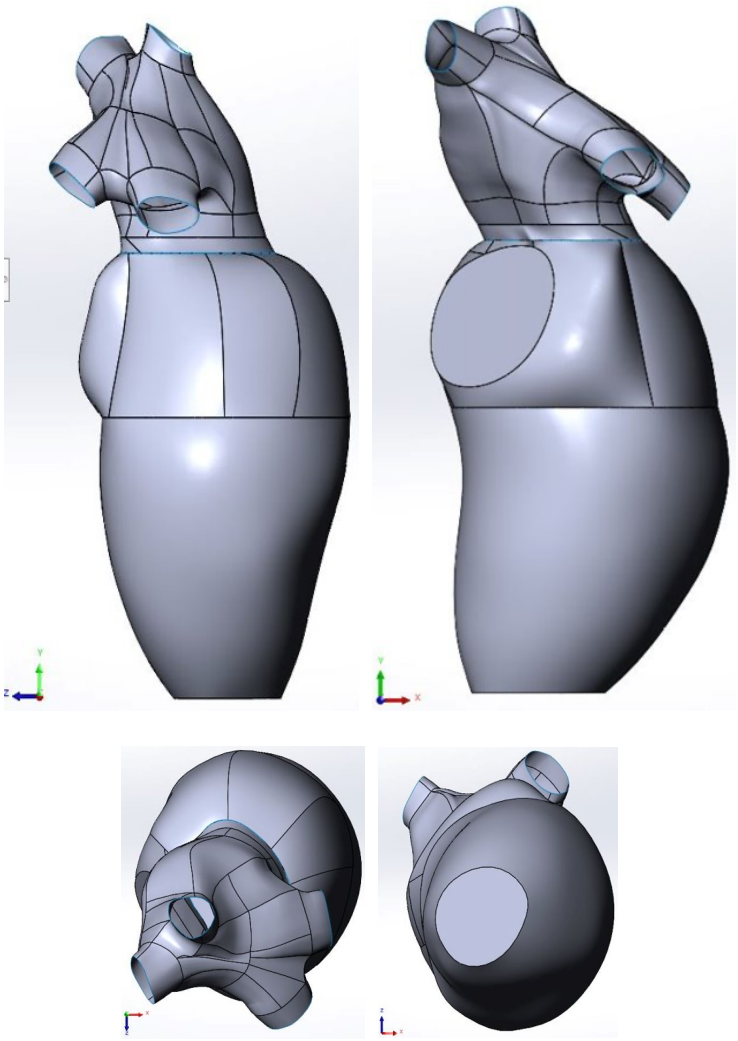

Figure 3.2.3: CAD model of left heart; left atrium, mitral valve, and left ventricle.

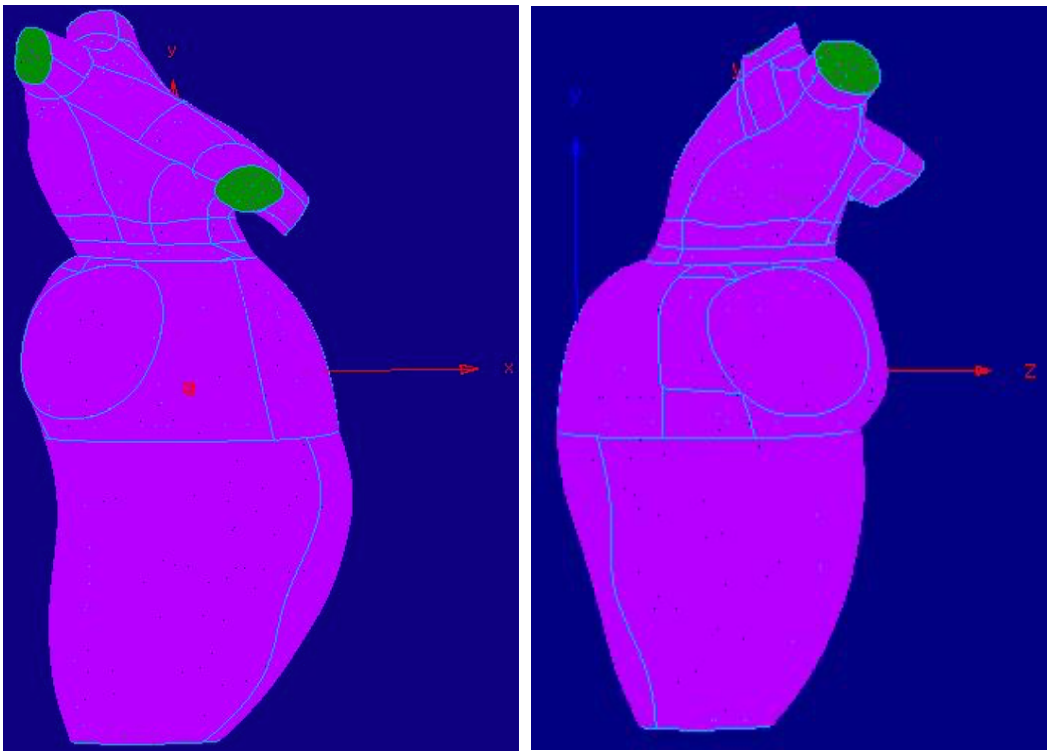

Figure 3.2.4: Meshed model of the full left heart model.

Table 3.2.1: Mesh element sizes assessed for optimal simulation convergence.

	LV & LA Mesh Size, mm	Mitral Valve Mesh Size, mm	Element Size
Main	1.0	0.35	3,034,793
Fine	0.7	0.35	5,094,754
Medium fine	0.65	0.35	9,118,203
Super fine	0.5	0.35	13,075,301

Table 3.2.2: Boundary Conditions applied in ANSYS fluid simulation.

Parameter	Value	Note
Fluent Launcher Settings	3D; Double Precision; Parallel Processing	
Solver	Pressure-Based	
Time	Steady	
Viscous Model	K-epsilon (2eqn)	
Fluid Density	1060 kg/m3	*Blood property
Fluid Viscosity	0.004kg/m-s	*Blood property
Pressure Inlet	16665.3 Pa	*Applied at bottom of Left Ventricle
Pressure Outlet	666.6 Pa	*Applied at Pulmonary Veins
Pressure Outlet	15998.7 Pa	*Applied at Aorta
Residual Convergence	1e-06	
Solution Initialization	Hybrid	
Number of Iterations	300	

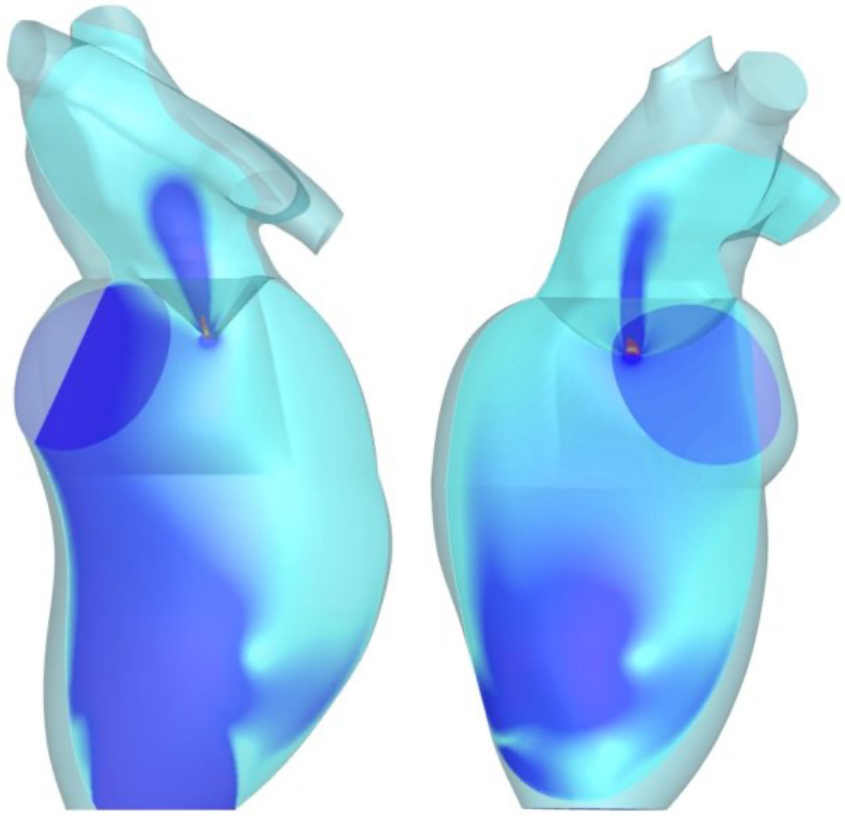

Figure 3.2.5: Image of left heart model post-processing. Short and long view of regurgitant flow through the orifice, respectively.

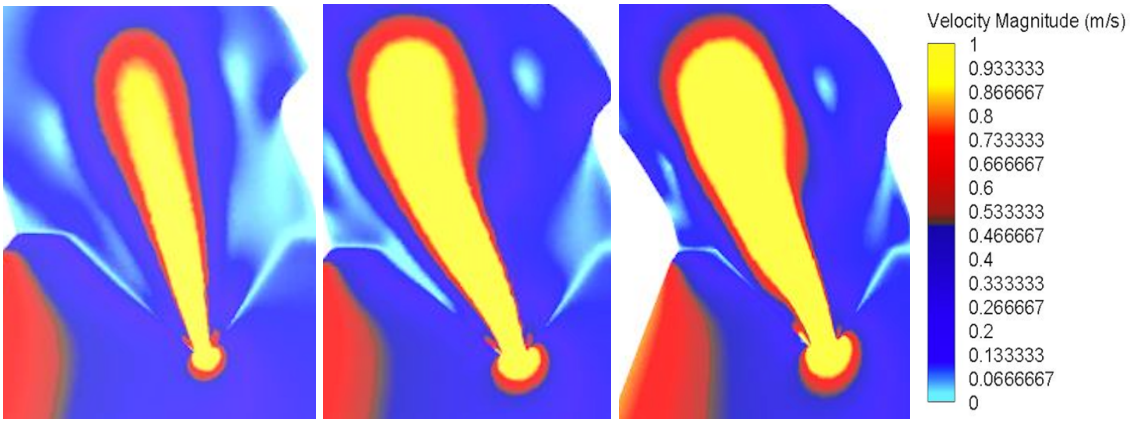

Figure 3.2.6: Native Mitral Valve velocity magnitude contours in the short-view displaying the regurgitant jet in the mild, moderate, and severe MR cases, respectively.

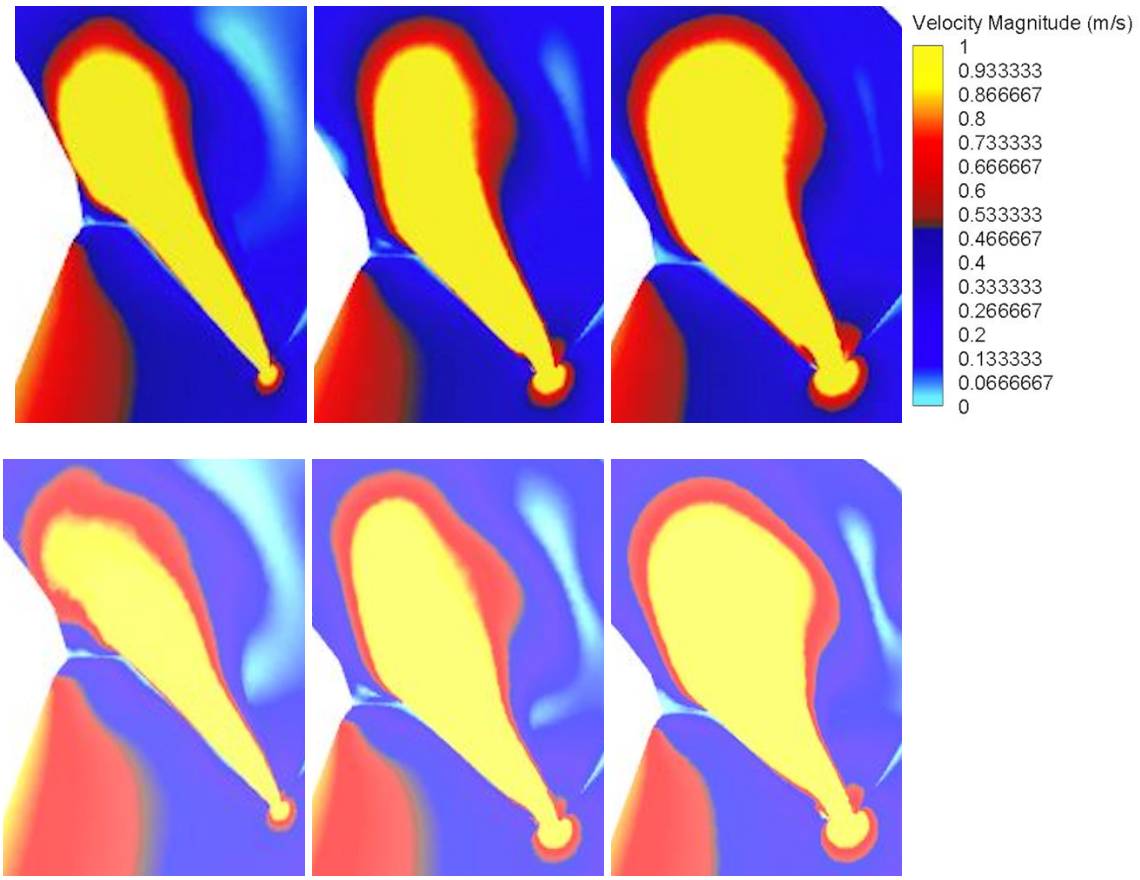

Figure 3.2.7: MitraClip Mitral Valve velocity magnitude contours in the short-view displaying the regurgitant jet in the mild, moderate, and severe MR cases, respectively, in both the back orifice (top row) and front orifice (bottom row).

3.3 Quantification of Mitral Regurgitation ; Modified Hemielliptic PISA

Calculated flows were compared to actual flow rate values found in the simulation by the sum found at the pulmonary veins. Measurements for modified PISA quantification were taken from the velocity magnitude contours in both views. As shown in Figure 3.3.1, the radial measurement of the PISA shell was taken from the most narrow point of regurgitant flow to the aliasing velocity (red-blue color shift). The angle of the

PISA shell (Figure 3.3.2) was measured from the full PISA shell shown, not only considering 180 degrees.

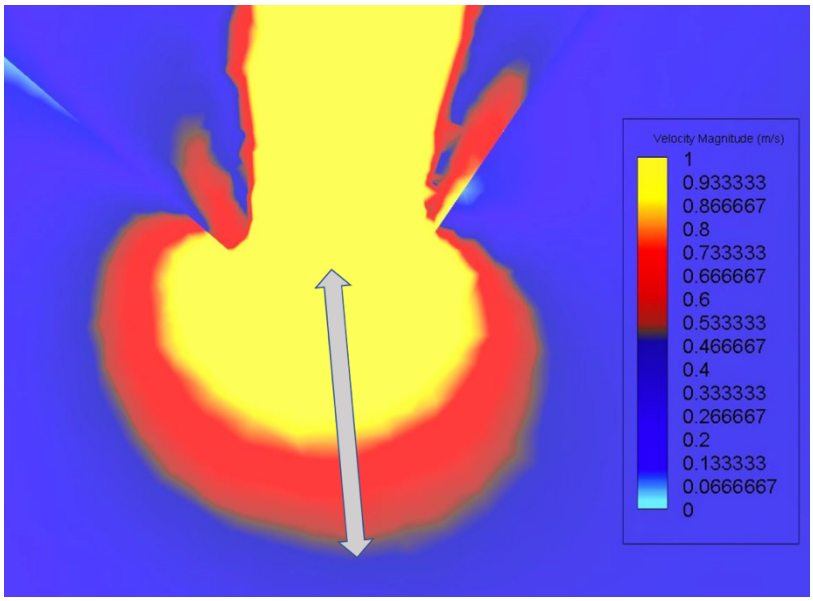

Figure 3.3.1: Computational simulation PISA radius (r) measurement.

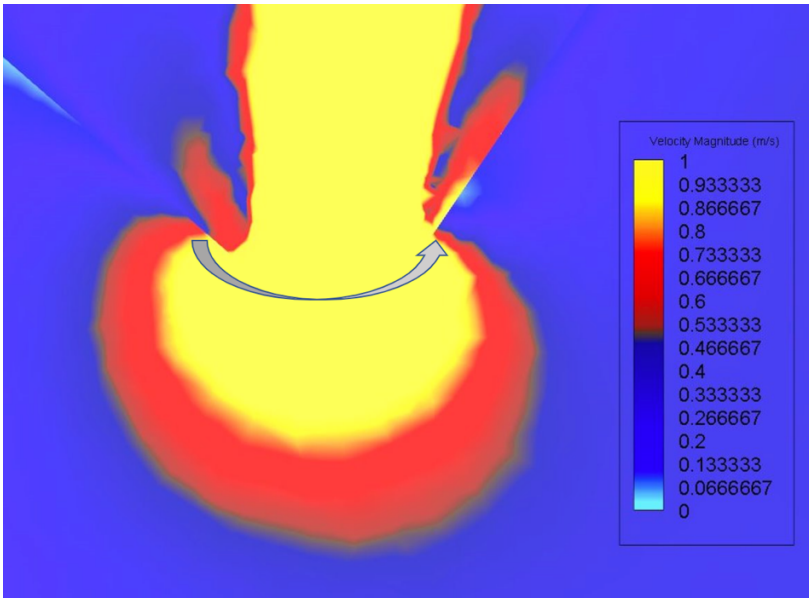

Figure 3.3.2: Computational simulation PISA shell angle measurement.

Table 3.3.1: Displays computational simulation Native Mitral Valve data regarding severity case. Regurgitant Orifice Flow Rate, Effective Regurgitant Orifice Area, Regurgitant Orifice Flow Rate Total of short and long view data, Effective Regurgitant Orifice Area Total of short and long view data, Actual Flow Rate, and respective Percentage Errors of each compared to the Actual Flow Rate.

	NMV Mild		NMV Moderate		NMV Severe	
	Short View	Long View	Short View	Long View	Short View	Long View
Regurgitant Orifice Flow Rate $_{ml/beat}$	6.98	10.1	15.6	24.2	31.7	40.9
EROA $_{mm^2}$	0.73	1.05	1.63	2.39	2.94	3.80
Percentage Error $_{\%}$	54.4	33.7	56.8	33.1	54.5	41.2
Regurgitant Orifice Flow Rate, Total $_{ml/beat}$	17.1		39.9		72.5	
EROA, Total $_{mm^2}$	1.779		4.019		6.741	
Flow Rate, Actual $_{ml/beat}$	15.3		36.2		69.5	
Percentage Error, Total $_{\%}$	11.7		10.2		4.3	

Table 3.3.2: Displays computational simulation Mitral Clip Mitral Valve data regarding severity case. Regurgitant Orifice Flow Rate, Effective Regurgitant Orifice Area, Regurgitant Orifice Flow Rate Total of short and long view data, Effective Regurgitant Orifice Area Total of short and long view data, Actual Flow Rate, and respective Percentage Errors of each compared to the Actual Flow Rate.

	MCMV Mild; Front Orifice		MCMV Mild; Back Orifice		MCMV Moderate; Front Orifice		MCMV Moderate; Back Orifice		MCMV Severe; Front Orifice		MCMV Severe; Back Orifice	
	Short View	Long View	Short View	Long View	Short View	Long View	Short View	Long View	Short View	Long View	Short View	Long View
Regurgitant Orifice Flow Rate $_{ml/beat}$	3.82	3.86	4.25	4.46	10.5	14.6	11.1	12.3	16.3	22.4	19.1	22.4
EROA $_{mm^2}$	0.41	0.46	0.46	0.47	1.14	1.44	1.16	1.18	1.73	2.17	2.04	1.95
Percentage Error $_{\%}$	77.8	77.6	74.1	75.3	77.4	68.7	76.3	73.6	79.4	71.7	75.8	74.3
Regurgitant Orifice Flow Rate, Total $_{ml/beat}$	16.2				48.6				78.3			
EROA, Total $_{mm^2}$	1.802				4.889				7.889			
Flow Rate, Actual $_{ml/beat}$	17.2				46.7				79.2			
Percentage Error, Total $_{\%}$	5.8				4.1				1.1			

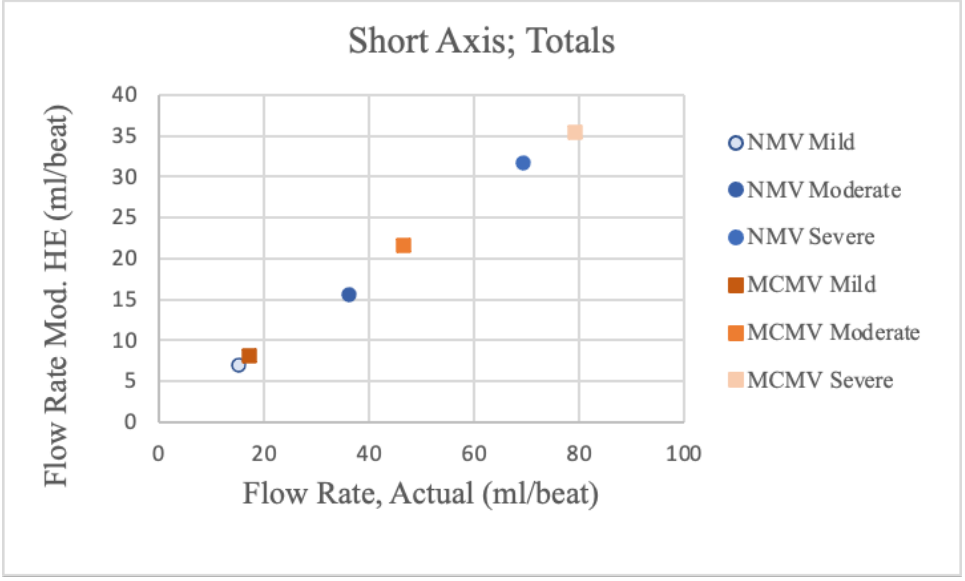

Figure 3.3.3: Correlation between calculated flow rates (Regurgitant Orifice Flow Rate) and Actual Flow Rate in the short-view.

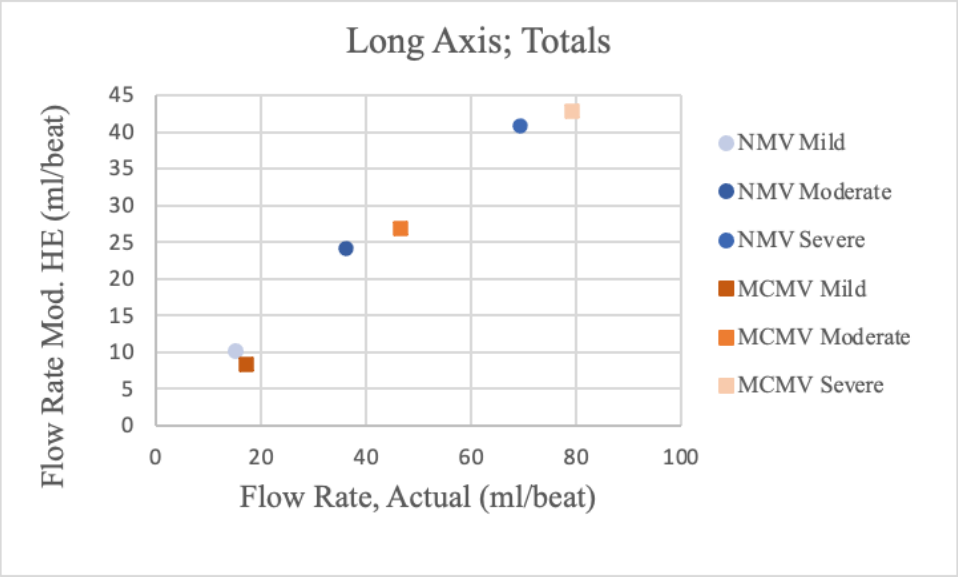

Figure 3.3.4: Correlation between calculated flow rates (Regurgitant Orifice Flow Rate) and Actual Flow Rate in the long-view.

Chapter Four: Discussion

4.1 Ex vivo Testing

During ex vivo testing, methods used regarding the steady flow and pulsatile flow system were continuously improved, as well as testing methods regarding the use of the Philips iE33 ultrasound machine and quantifying MR. A steady flow system proved to be a practical preliminary practice in ex vivo testing, however, the MR jet was often difficult to find when using Color Doppler as ultrasound machines are geared towards evaluating pulsatile flows.

Throughout the test trials of the Full Cardiac Simulator, this pulsatile flow proved to be noteworthy, clearly demonstrating its future potential. Although minimal data regarding MR was obtained during these test trials, necessary modifications were made and notable areas of improvements were found. The Full Cardiac Simulator shows the possibilities of a more comprehensive ex vivo testing methodology that may be used not only for the assessment of MR, but for the evaluating numerous cardiovascular diseases.

4.2 Computational Fluid Dynamics

PISA quantification is heavily dependent on the aliasing velocity (i.e. the color shift shown in the simulated contours). This study considered the range of velocity

magnitude in the plane of interest with a maximum of 1 m/s and a minimum of zero. 16 increments were set to the color map as this is also the case regarding Color Doppler and Nyquist limit shifting with the Philips iE33 ultrasound machine. Shifting the baseline aliasing velocity was practiced to more clearly view the PISA shell for an accurate measurement of the radius. Specific coordinate planes were inserted through each valve directly in the center of the short and long view of the orifice.

In all six cases evaluated, values obtained using the modified hemielliptic PISA method consistently showed to underestimate the regurgitant flow in both the short and long view of the orifice compared to the actual total regurgitant flow found at the pulmonary veins. Furthermore, measurements taken in the long view continually showed to underestimate regurgitant flow even more so than measurements take in the short view. The percentage error shows to be greater than 30% in each view of every case, clearly showing a substantial difference between the calculated and actual flow rate. In a clinical setting, this would lead to an inaccurate diagnosis of MR severity, eventually leading to improper treatment. Through computational simulations, improvements that can be made in clinical measurement techniques were also displayed. Through being able to control the anatomy and flow in these simulations, it can be shown where optimal transducer placement may be in order to get the most accurate reading of PISA during TTE.

4.3 Study Limitations & Future Works

4.3.1 Ex vivo Testing

Though the importance of having a full comprehensive cardiac simulator is evident, there were certain impediments encountered when trying to measure MR. It is prominent that all connection points of the simulator are secure as to ensure minimal leakage. This is dependent on quality of materials, especially in regards to the porcine heart used as a test subject. Ensuring this secure connection continued show difficulty at the superior vena cava and pulmonary veins, as they were cut rather short by the source which they were obtained from. Furthermore, cuts are often made on the heart itself by these sources, indicating more areas for outflow. Apical connection could further be improved by creating higher quality cannulas and using tubing at this connection that is highly flexible, as to not put any strain on the heart and this connection point. Future studies may also use a microscopic camera to insert into the pulmonary vein to evaluate the condition and make necessary cuts on the mitral valve to enact MR without opening the LA to do so.

4.3.2 Computational Fluid Dynamics

With PISA measurement accuracy being most prominent in MR quantification, it continues to show the importance of the aliasing velocity setting during this time. With a high aliasing velocity, PISA will be small; with a low aliasing velocity, PISA will be large. (9) Aliasing velocity is based on the set Nyquist limit, which is equal to the pulse repetition frequency (PRF)/2. In order to continue to evaluate PISA with the use of

computational fluid dynamics, aliasing velocity and its implementation in a clinical setting should continue to be further investigated. PISA and aliasing velocity may also be further investigated through the use of fluid-structure interaction (FSI).

Chapter Five: Conclusions

This study aimed to show the importance of further development in methods used to quantify the severity of mitral regurgitation. Calculated flow rates throughout the native mitral valve cases and the MitraClip mitral valve cases showed to underestimate regurgitant flow in the short view of the orifice, and even further underestimate the flow in the long view of the orifice compared to the actual regurgitant flow. Both native and MitraClip cases of calculated flow rates in both views also correlated rather closely. Computational simulations proved to be of significance in testing new mathematical models and how they may further be executed in a clinical setting. Continuing to improve clinical techniques used to obtain accurate measurements, mathematical models used for quantification, computational fluid dynamic methods for patient specific simulations, and the innovation of a Full Cardiac Simulator to advance ex vivo testing, exemplify the many factors that need to be accounted for when attempting the quantify mitral regurgitation as accurately as possible.

References

1Apostolakis, E. E., & Baikoussis, N. G. (2009). Methods of estimation of mitral valve regurgitation for the cardiac surgeon. *J Cardiothorac Surg*, *4*, 34. https://doi.org/10.1186/1749-8090-4-34

2Athappan, G., Raza, M. Q., & Kapadia, S. R. (2016). MitraClip Therapy for Mitral Regurgitation: Primary Mitral Regurgitation. *Interv Cardiol Clin*, *5*(1), 71-82. https://doi.org/10.1016/j.iccl.2015.08.006

3Caballero, A., Mao, W., McKay, R., Hahn, R. T., & Sun, W. (2020). A Comprehensive Engineering Analysis of Left Heart Dynamics After MitraClip in a Functional Mitral Regurgitation Patient [Original Research]. *Frontiers in Physiology*, *11*(432). https://doi.org/10.3389/fphys.2020.00432

4Delgado, V., Tops, L. F., Schuijf, J. D., de Roos, A., Brugada, J., Schalij, M. J., Thomas, J. D., & Bax, J. J. (2009). Assessment of mitral valve anatomy and geometry with multislice computed tomography. *JACC Cardiovasc Imaging*, *2*(5), 556-565. https://doi.org/10.1016/j.jcmg.2008.12.025

5Feldman, T., Fernandes, E., & Levisay, J. P. (2018). Transcatheter mitral valve repair/replacement for primary mitral regurgitation. *Annals of cardiothoracic surgery*, *7*(6), 755-763. https://doi.org/10.21037/acs.2018.07.04

6Fujii, H., Kibira, S., Izumi, C., Saito, T., Ryabikov, A., & Miura, M. (2001). Hemielliptic proximal isovelocity surface area method modified for clinical application: more accurate quantification of mitral regurgitation in Doppler echocardiography. *Japanese circulation journal*, *65*, 820-826.

7Grayburn, P. A., Weissman, N. J., & Zamorano, J. L. (2012). Quantitation of Mitral Regurgitation. *Circulation*, *126*(16), 2005-2017. https://doi.org/10.1161/CIRCULATIONAHA.112.121590

8Imbrie-Moore, A. M., Paulsen, M. J., Zhu, Y., Wang, H., Lucian, H. J., Farry, J. M., MacArthur, J. W., Ma, M., & Woo, Y. J. (2021). A novel cross-species model of Barlow's disease to biomechanically analyze repair techniques in an ex vivo left heart simulator. *J Thorac Cardiovasc Surg*, *161*(5), 1776-1783. https://doi.org/10.1016/j.jtcvs.2020.01.086

9Lancellotti, P., Tribouilloy, C., Hagendorff, A., Popescu, B. A., Edvardsen, T., Pierard, L. A., Badano, L., Zamorano, J. L., & On behalf of the Scientific Document Committee of the European Association of Cardiovascular Imaging: Thor Edvardsen, O. B. B. C. E. D. R. D. M. G. P. L. D. M. K. (2013). Recommendations for the echocardiographic assessment of native valvular regurgitation: an executive summary from the European Association of Cardiovascular Imaging. *European Heart Journal - Cardiovascular Imaging*, *14*(7), 611-644. https://doi.org/10.1093/ehjci/jet105

10Leopaldi, A. M., Wrobel, K., Speziali, G., van Tuijl, S., Drasutiene, A., & Chitwood, W. R., Jr. (2018). The dynamic cardiac biosimulator: A method for training physicians in beating-heart mitral valve repair procedures. *J Thorac Cardiovasc Surg*, *155*(1), 147-155. https://doi.org/10.1016/j.jtcvs.2017.09.011

11Mao, W., Caballero, A., Hahn, R. T., & Sun, W. (2020). Comparative quantification of primary mitral regurgitation by computer modeling and simulated

echocardiography. *Am J Physiol Heart Circ Physiol*, *318*(3), H547-h557. https://doi.org/10.1152/ajpheart.00367.2019

12Moraldo, M., Cecaro, F., Shun-Shin, M., Pabari, P. A., Davies, J. E., Xu, X. Y., Hughes, A. D., Manisty, C., & Francis, D. P. (2013). Evidence-based recommendations for PISA measurements in mitral regurgitation: systematic review, clinical and in-vitro study. *International Journal of Cardiology*, *168*(2), 1220-1228. https://doi.org/https://doi.org/10.1016/j.ijcard.2012.11.059

13O'Gara Patrick, T., Grayburn Paul, A., Badhwar, V., Afonso Luis, C., Carroll John, D., Elmariah, S., Kithcart Aaron, P., Nishimura Rick, A., Ryan Thomas, J., Schwartz, A., & Stevenson Lynne, W. (2017). 2017 ACC Expert Consensus Decision Pathway on the Management of Mitral Regurgitation. *Journal of the American College of Cardiology*, *70*(19), 2421-2449. https://doi.org/10.1016/j.jacc.2017.09.019

14Otto, C. M. (2003). Timing of surgery in mitral regurgitation. *Heart (British Cardiac Society)*, *89*(1), 100-105. https://doi.org/10.1136/heart.89.1.100

15Paulsen, M. J., Imbrie-Moore, A. M., Wang, H., Bae, J. H., Hironaka, C. E., Farry, J. M., Lucian, H. J., Thakore, A. D., MacArthur, J. W., Cutkosky, M. R., & Woo, Y. J. (2020). Mitral chordae tendineae force profile characterization using a posterior ventricular anchoring neochordal repair model for mitral regurgitation in a three-dimensional-printed ex vivo left heart simulator. *Eur J Cardiothorac Surg*, *57*(3), 535-544. https://doi.org/10.1093/ejcts/ezz258

16The Practice of Clinical Echocardiography - Otto.pdf.

17Schmidt, F. P., von Bardeleben, R. S., Nikolai, P., Jabs, A., Wunderlich, N., Münzel, T., Hink, U., & Warnholtz, A. (2013). Immediate effect of the MitraClip procedure on mitral ring geometry in primary and secondary mitral regurgitation. *Eur Heart J Cardiovasc Imaging*, *14*(9), 851-857. https://doi.org/10.1093/ehjci/jes293

18Textbook of Clinical Echocardiography - Otto.pdf.

19Thavendiranathan, P., Phelan, D., Collier, P., Thomas James, D., Flamm Scott, D., & Marwick Thomas, H. (2012). Quantitative Assessment of Mitral Regurgitation. *JACC: Cardiovascular Imaging*, *5*(11), 1161-1175. https://doi.org/10.1016/j.jcmg.2012.07.013

20Wu, S., Chai, A., Arimie, S., Mehra, A., Clavijo, L., Matthews, R. V., & Shavelle, D. M. (2018). Incidence and treatment of severe primary mitral regurgitation in contemporary clinical practice. *Cardiovasc Revasc Med*, *19*(8), 960-963. https://doi.org/10.1016/j.carrev.2018.07.021

21Zhu, Y., Imbrie-Moore, A. M., Paulsen, M. J., Priromprintr, B., Park, M. H., Wang, H., Lucian, H. J., Farry, J. M., & Woo, Y. J. (2021). A Novel Aortic Regurgitation Model from Cusp Prolapse with Hemodynamic Validation Using an Ex Vivo Left Heart Simulator. *J Cardiovasc Transl Res*, *14*(2), 283-289. https://doi.org/10.1007/s12265-020-10038-z

22Zoghbi, W. A., Adams, D., Bonow, R. O., Enriquez-Sarano, M., Foster, E., Grayburn, P. A., Hahn, R. T., Han, Y., Hung, J., Lang, R. M., Little, S. H., Shah, D. J., Shernan, S., Thavendiranathan, P., Thomas, J. D., & Weissman, N. J. (2017). Recommendations for Noninvasive Evaluation of Native Valvular Regurgitation:

A Report from the American Society of Echocardiography Developed in Collaboration with the Society for Cardiovascular Magnetic Resonance. *Journal of the American Society of Echocardiography*, *30*(4), 303-371. https://doi.org/10.1016/j.echo.2017.01.007

23Zoghbi, W. A., Enriquez-Sarano, M., Foster, E., Grayburn, P. A., Kraft, C. D., Levine, R. A., Nihoyannopoulos, P., Otto, C. M., Quinones, M. A., Rakowski, H., Stewart, W. J., Waggoner, A., & Weissman, N. J. (2003). Recommendations for evaluation of the severity of native valvular regurgitation with two-dimensional and doppler echocardiography. *Journal of the American Society of Echocardiography*, *16*(7), 777-802. https://doi.org/https://doi.org/10.1016/S0894-7317(03)00335-3

Appendix A

Table A1: Phone call notes of discussions with Philips ultrasound technician on how to improve ultrasound images.

Call	Date	Notes
#1	3/17/2021	• We have x51 transducer • Steady flow may be difficult to test on • Particles may be problem for clear image; adds density • Want transducer on LV • Contrast preset designed for infused bubbles; keeps beam from bursting ultrasound bubbles • Low flow = want low Nyquist ; higher pressure = increase Nyquist • Fluid added to RA/RV will help with imaging • Apical view on LV of patient
#2	7/22/2021	• Better images in trial 7/19/2021 • Depth is too deep; decrease this • Need to find 2D anatomy first before color doppler • Transducer posterior to aortic valve for 4 chamber valve • Bring more posterior to better see MV

Table A2: Experimental testing notes taken throughout ex vivo testing.

Trial	Date	Notes
Trial 1	2/17/2021	• Put together flow system • Tested connection points
Trial 2	2/24/2021	• Tested connection of pig heart to flow system • Practice with ultrasound machine; getting familiar with settings and transducer placement on the heart

Trial 3	3/3/2021	• Pressure at 60mmhg at 5:22pm • Pressure at 75mmhg at 5:40pm • Pressure at 26mmhg at 6:12pm • Flow meter only worked once; read at 2.18 L/min
Trial 4	3/7/2021	• After image 11 cut more valve • Flow rate measured at 2.6 L/min • Flow rate measured at 5.4 L/min at 2:03pm • Too many particles were used • Pressure 48.7mmhg @ 12:13pm • Pressure 46.5mmhg @ 1:22pm • Pressure 40.1mmhg @ 1:33pm
Trial 5	3/10/2021	• Pressure 46.1mmhg at 10:19am • Pressure 43.4 at 10:24am • Pressure 46.6mmhg at 10:28am • Pressure at 45.4mmhg at 11:01am • Pressure at 45.4mmhg at 11:14am • Pressure at 50.6mmhg at 11:56am • Pressure at 44.1mmhg at 12:21pm • Pressure at 48.9mmhg at 12:25pm
Trial 6	3/12/2021	• Start with a small amount of PIV particles • Flow rate measured at 5.3 L/min • Photos 1-6; No changes were made from Trial 2 • Added more PIV particles half way through; Cut more muscle • Flow rate measured at 9.4 L/min; Photos 7-17 • Added more particles • Flow rate measured at 8.6 L/min; Photos 18-22 • Flow rate measured at 9.5 L/min; Photos 23-39 • Change in heart position; now in vertical position • Flow rate measured at 9.01 L/min
Trial 7	3/18/2021	• Pressure 191mmhg at 3:45pm • Pressure 159mmhg at 3:55pm • Flow rate at 0.55 L/min at 3:45pm

		• Pressure 186mmhg at 3:45pm • Flow rate at 0.43 L/min at 3:55pm • Flow rate at 0.62 L/min at 4:15pm • Cutting 1 chordae at A2; suture • Can hear the jet flow difference • Aortic tear continued to get worse as time went on
Trial 8	3/19/2021	• Pressure 118.7mmhg at 6:57pm • Pressure 130.3mmhg at 7:01pm • Flow rate at 0.75 L/min at 6:54pm • Flow rate at 0.63 L/min at 6:55pm • Flow rate at 0.78 L/min at 7:40pm
Trial 9	3/20/2021	• Flow rate measured at 1.21 L/min @ 10:20am • Flow rate measured at 0.54 L/min @ 10:22am • Flow rate measured at 1.25 L/min @ 11:43am • Pressure 98mmhg @ 10:17 am • Pressure 63.1mmhg @ 10:23am • Pressure 91.2mmhg @ 11:43am • Pressure 138mmhg @ 11:57 am • Image 1 is without water sack • Image 32; used water sack for transducer
Trial 10	7/8/2021	• Test better transducer placement and Nyquist baseline shift to accurately see PISA jet
Trial 11	7/19/2021	• Cut RV off • Cut LA appendage off; next time suture this entirely • Septum thickness is roughly ½ inch thick; along with around LV • Apex is roughly 1 inch thick • “X” cut on apex to insert cannula; inside valve to create hole insertion • Cut MV through cannula insertion; mark at commissure from pressurized top • Cut on P2; cut on A2 is better; made jet halfway through leaflet • 4cm down from top is pump jet • 12cm down from top view is MV jet

		• Removal of RV to test transducer on LV
Trial 12	8/13/2021	• Need to pressure transducer tops • Need better stand for the system • Look at LVAD video and their cannulas • Create cannula with inner LV piece as well • Need fresh sheep or pig hearts; need to size connections down to ½ inch • Need flexible tubing • Need to create “Y” piece for pump connection • Need heart tray / stand system • Prep. hearts day before testing; with cuts and connection pieces • Need heart to be cold • Need to be able to easily slide tubing on to adapters
Trial 13	8/27/2021	• Biggest issue is connection at the pulmonary veins; difficult with the multiple connections and needing to suture; Sutures only holding up for so long • Still need better cannulas • Need custom tubing that is very flexible and does not put a pressure / strain on the connection to the heart

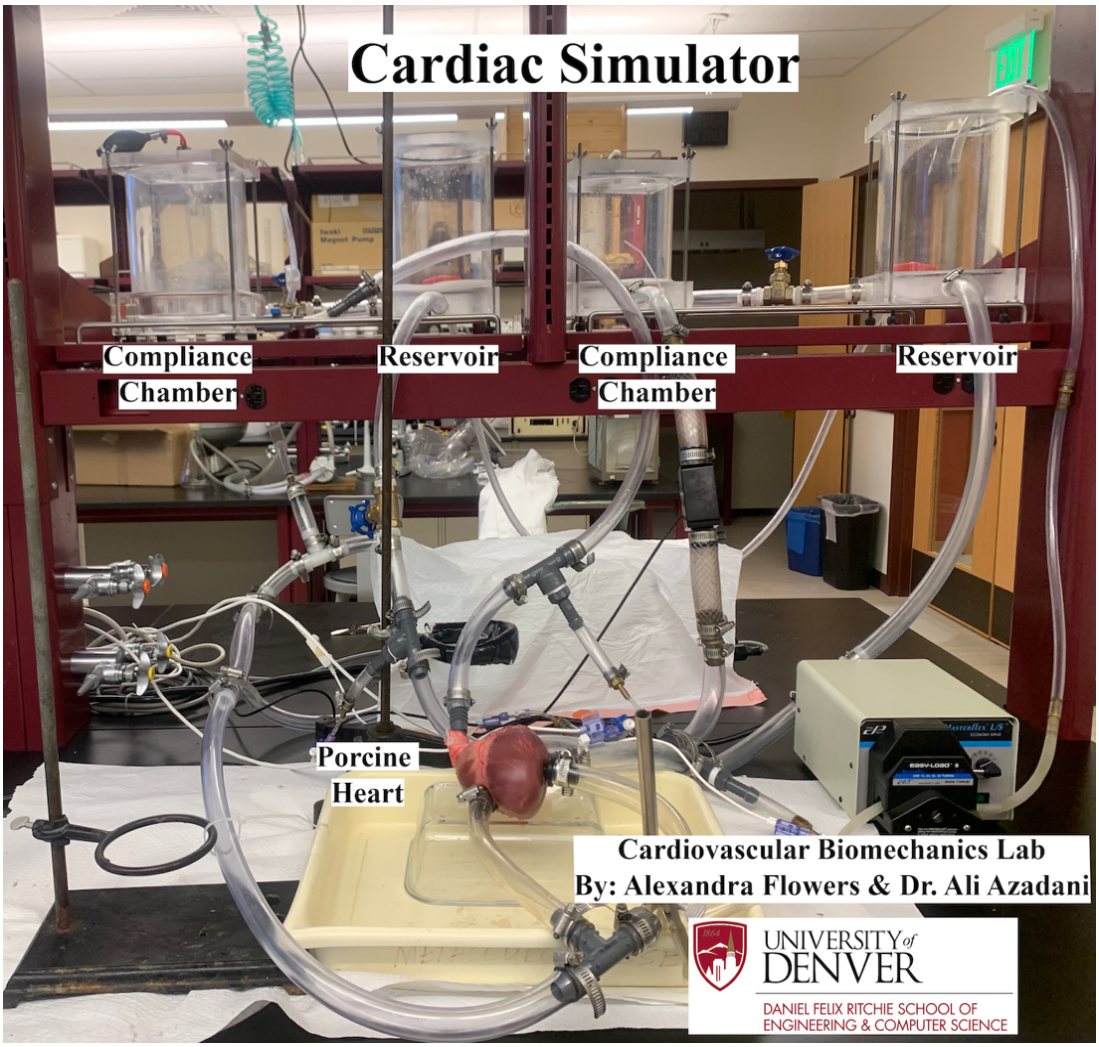

Figure A3: Full Cardiac Simulator. This image was used to help promote the work that we are able to do “in-house”, using numerous machines within our machine shop.